Biomechanical parameters of marram grass (*Calamagrostis arenaria*) for advanced modeling of dune vegetation

Viktoria Kosmalla[1], Oliver Lojek[1], Jana Carus[2], Kara Keimer[1], Lukas Ahrenbeck[1], Björn Mehrtens[1], David Schürenkamp[1], Boris Schröder[2,3], and Nils Goseberg[1,4]

[1]Technische Universität Braunschweig, LeichtweiSS-Institute for Hydraulic Engineering and Water Resources; Division of Hydromechanics, Coastal and Ocean Engineering; BeethovenstraSSe 51a, 38106 Braunschweig, Germany
[2]Technische Universität Berlin, Institute of Ecology; Department of Plant Ecology; RothenburgstraSSe 12, 12165 Berlin, Germany
[3]Berlin-Brandenburg Institute of Advanced Biodiversity Research; AltensteinstraSSe 6, 14195 Berlin, Germany
[4]Coastal Research Center; Joint Central Institution of Leibniz Universität Hannover and Technische Universität Braunschweig; MerkurstraSSe 14, 30419 Hannover, Germany

Correspondence: Viktoria Kosmalla (v.kosmalla@tu-braunschweig.de)

Abstract. This study investigates the biomechanical properties of marram grass (*Calamagrostis arenaria*, formerly *Ammophila arenaria*) over a 12-month period on the island of Spiekeroog, Germany, to enhance the modeling of coastal dune dynamics. The research reveals significant seasonal variations in the stiffness and Young's modulus of the vegetation, with higher values observed in winter, indicating increased mechanical resistance important for dune stability during storm events. In summer, increased flexibility and density are prominent, enhancing dune accretion. To account for these dynamics, the study emphasizes the importance of incorporating seasonally adjusted parameters into models, particularly accounting for the increased horizontal density, the presence of flower stems in summer, and the longer leaf lengths in winter. The differentiation among plant parts is highlighted, with flower stems providing the highest structural support due to their greater stiffness, while leaves contribute more to flexibility and dynamic responses. Interestingly, the minimal differences between green and brown leaves suggest that these can be treated similarly in modeling efforts, simplifying parametrization without compromising accuracy. Additionally, the study found no consistent evidence that wind exposure significantly affects the biomechanical properties of marram grass, suggesting that wind influence may not need to be factored into biomechanical models. The results also demonstrate that the biomechanical properties of marram grass are broadly transferable between fixed and dynamic dune systems, supporting their applicability across various coastal environments. The key outcome of this research is the detailed compilation of the biomechanical traits of marram grass's aboveground vegetation, reflecting the seasonal dynamics found in dune processes, which will serve as a valuable resource for future modeling efforts of dune vegetation and their surrogates.

1 Introduction

Coastal dunes are among the most dynamic ecosystems on Earth, shaped by the interplay between physical and biological processes (Hesp, 2002; Hacker et al., 2012; Zarnetske et al., 2015; Strypsteen et al., 2019).They act as natural coastal barriers, mitigating storm impacts and protecting inland areas from flooding (Martínez and Psuty, 2004; Feagin et al., 2015; Ruggiero et al., 2018). Besides their protective function, dunes support high ecological diversity and provide essential ecosystem services, including freshwater provision and sediment stabilization (Martínez and Psuty, 2004; Everard et al., 2010; Barbier et al., 2011; Röper et al., 2013; Ruggiero et al., 2018). The dynamic interactions between physical and biological processes result in high spatio-temporal complexity within dune systems (de Vries et al., 2012). Understanding the dynamics of dune erosion and accretion is essential, as these processes determine the safety level of coastal dunes against hinterland flooding due to storm surges (González-Villanueva et al., 2023), forming the basis for their integration as ecosystem-based coastal defense measures (de Vries et al., 2012; Feagin et al., 2015; de Battisti, 2021). Both short-term changes in dune morphology from individual storm events, such as erosion and deposition of sediment, and long-term trends influenced by sea level rise, sediment supply, human activity, and the stabilizing effects of vegetation (Keijsers et al., 2016; Gao et al., 2020; Hovenga et al., 2021; González-Villanueva et al., 2023) are crucial for accurately assessing and managing the protective functions of coastal dunes (Keijsers et al., 2016; Gao et al., 2020; Farrell et al., 2023; Husemann et al., 2024).

Coastal dunes, unlike engineered structures, adapt dynamically through natural processes like sediment transport and vegetation growth, enabling post-storm recovery and resilience to sea-level rise (van Gent et al., 2008; van IJzendoorn et al., 2021; Mehrtens et al., 2022, 2023). Dynamic dune management supports these processes while promoting biodiversity and ecosystem services. Climate change impacts dune vegetation, altering species distribution and traits (Carter, 1991; Duarte et al., 2013; Gao et al., 2020; de Battisti, 2021; Biel and Hacker, 2021). Carter (1991), e.g., stated that species tolerant to higher temperatures, drought, and sand burial may become more dominant in the future.

Understanding these vegetation development and characteristics is crucial, as plants not only shape dune formation but also provide essential ecosystem services, such as carbon sequestration (Barbier et al., 2011). To simulate the interactions between vegetation, sand, wind, and water in dune environments, various numerical models, e.g., DUBEVEG (Keijsers et al., 2016; Husemann et al., 2024), AeoLIS (van Westen et al., 2024), and XBeach implementations (Schweiger and Schuettrumpf, 2021), as well as physical models have been developed. However, the accuracy of these models strongly depends on high-quality datasets derived from field observations, which, to date, have not been systematically collected for the specific biomechanical properties of dune vegetation. In physical experiments, dune vegetation is often either neglected (van Gent et al., 2007; Tomasicchio et al., 2011; Figlus et al., 2011; Mehrtens et al., 2024) or represented using real vegetation (Figlus et al., 2014; de Battisti and Griffin, 2020; Silva et al., 2016; Maximiliano-Cordova et al., 2019; Feagin et al., 2019) or simplistic mimics such as wooden dowels (Bryant et al., 2019; Kobayashi et al., 2013; Türker et al., 2019), which presents challenges in terms of scalability and accurately replicating biomechanical properties of the vegetation (Garzon et al., 2021). Most vegetation modeling efforts in NbS for coastal protection have focused on salt marsh vegetation, aiming to improve the representation of plant physiology, morphology, and hydrology (Liu et al., 2021; Keimer et al., 2024). These models seek to capture the complex feedback mechanisms between vegetation and the environment, including the effects of plant traits on sediment transport, wind erosion, and water availability. In salt marsh ecosystems, vegetation density and mechanical properties such as stiffness have been identified as key factors influencing wave attenuation and shoreline stabilization (Shepard et al., 2011). However, salt marsh plants differ significantly from dune vegetation in terms of morphology, biomechanical properties, and response to hydrodynamic and aeolian forces. While salt marsh plants typically exhibit high flexibility and resistance to hydrodynamic forces

(Vuik et al., 2017; Bouma et al., 2014), dune grasses primarily contribute to sediment stabilization through their aboveground stiffness and extensive rhizome networks (Zarnetske et al., 2012; Figlus et al., 2022). Consequently, the transferability of existing vegetation parameterizations from salt marshes to dune environments is therefore limited, necessitating a more refined biomechanical representation of dune vegetation in coastal models. Despite the recognized importance of plant morphology, research on the biomechanical role of dune vegetation remains limited. On a cellular level, differences between plant components have been highlighted, with stems providing structural stability, while leaves exhibit greater flexibility and resistance to wind exposure (Chergui et al., 2017). Given these functional differences, a biomechanical characterization of dune vegetation that explicitly accounts for the mechanical roles of different plant components is essential to improve its representation in coastal models. However, most biomechanical studies on coastal vegetation to date have focused on plant species commonly found in salt marshes, seagrass meadows, or mangrove forests. Several studies, for instance, have employed three-point bending tests for investigating the biomechanics of salt marsh vegetation, assessing seasonal and species-specific differences (see Table A1 in the Appendix). In contrast, dune plants, such as European beachgrass, marram grass (*Calamagrostis arenaria*, formerly *Ammophila arenaria*, hereafter referred to as marram grass), have received much less attention, despite its critical role in dune stabilization and protection (Feagin et al., 2015; Davidson et al., 2020; de Battisti and Griffin, 2020). De Jong et al. (2014) explicitly emphasized the lack of research and highlighted the importance of studying vegetation development, particularly regarding density of cover and rooting depth; since then, little further research has appeared to fill the gap, and a better understanding of the biomechanics of dune vegetation remains crucial for improving modeling efforts.

Field data from the literature provide valuable insights into the characteristics of marram grass, though their interpretation is often complicated by inconsistent terminology and missing methodological descriptions. Previous studies have primarily focused on geometric and external plant traits, while biomechanical properties remain largely understudied. Histological examinations have been conducted by Andrade et al. (2021) and Chergui et al. (2017), and a review by McGuirk et al. (2022) summarizes current knowledge on the role of vegetation in dune dynamics, including quantitative studies on marram grass. A comprehensive overview of key parameters, such as growth height, horizontal density, and belowground biomass, is provided in Table A2 in the Appendix.

While these parameters are essential for developing accurate surrogate models, which we depict as non-withering, permanent laboratory replacement structures derived from in-situ characteristics of live plants, they primarily address geometric and external characteristics rather than the mechanical properties that determine how vegetation interacts with environmental forces. Studies such as Bouma et al. (2013) have demonstrated the importance of traits like shoot stiffness, shoot density, and shoot length in influencing the intensity and scale of vegetation-environment interactions, particularly in salt marsh ecosystems. However, there is currently limited knowledge on the mechanical properties of marram grass, such as flexibility and stiffness, which are vital for understanding its impact on dune stability and resilience to environmental stressors like wind or water flow. A better understanding of these mechanical traits is essential for assessing the contribution of dune vegetation to sediment stabilization and ecosystem resilience.

Vegetation in coastal ecosystems, such as salt marshes, exhibits marked seasonality in its traits. For example, during the summer, plant length and density significantly increase, while in the winter, the stiffness of the vegetation is greater and the outer diameter smaller (Vuik et al., 2017; Foster-Martinez et al., 2018; Keimer et al., 2024; Li et al., 2024). The effects of seasonality and vitality on vegetation traits can significantly impact their biomechanical properties, which in turn may influence dune stability and resilience to environmental stressors (Baas and Nield, 2010; de Jong et al., 2014; Biel and Hacker, 2021). Similarly, dune dynamics also follow seasonal patterns. Dunes typically experience erosion during winter and accretion during summer, leading to cyclic variations in dune morphology (Montreuil et al., 2013; Pye and Blott, 2016; Rader et al., 2018). These processes are driven by seasonal variations in wind and wave action, which shape the dune landscape. Although there is limited specific information on the seasonality of dune vegetation traits, it is known that marram grass has adapted to these dynamic processes. Regular sand burial is essential for its healthy growth, and without it, growth rates and relative abundance decrease significantly (Maun, 1998; Bonte et al., 2021), indicating an "escape" mechanism against certain nematode species (van der Putten and Troelstra, 1990; Bonte et al., 2021). During winter, the extensive root system of marram grass plays a crucial role in stabilizing the dunes by enhancing sediment properties, such as porosity, shear strength, and slope stability, thus reducing erosion and preventing uprooting during storm surges (Davidson et al., 2020; Walker and Zinnert, 2022). These interactions between seasonal vegetation traits and dune processes highlight the importance of incorporating seasonal variations into studies of dune vegetation properties to improve our understanding of their role in coastal defense.

In addition to seasonal influences, dune vegetation is subjected to external mechanical forces, such as wind or hydrodynamic loads, which can impact plant growth and biomechanical properties (Puijalon et al., 2005, 2011; Gardiner et al., 2016; Telewski, 2016; Du and Jiao, 2020; Kouhen et al., 2023). Plants respond to mechanical stress through different adaptive strategies, primarily classified as avoidance (minimizing frontal area) or tolerance (maximizing resistance to breakage). Species following the avoidance strategy tend to exhibit higher bending stiffness (Puijalon et al., 2011). Understanding these strategies is crucial for biomechanical characterization, as they determine how plants interact with environmental forces such as wind and waves. However, most studies on wind-induced biomechanical adaptations have focused on woody vegetation, such as trees, whereas their applicability to dune vegetation remains largely unclear. Given the significant role of wind in coastal environments, it is essential to investigate how dune vegetation responds to wind-induced mechanical stresses to improve our understanding of its biomechanical behavior.

Beyond mechanical forces, soil characteristics also shape vegetation properties. As dunes develop, changes in soil composition influence vegetation cover over the long-term (Isermann, 2011). In Europe, dune succession is often classified into white dunes, which are younger, more dynamic systems with active sand movements, and gray dunes, which are older, more stabilized formations with increased organic matter content (Isermann and Cordes, 1997). However, such classifications are not universally applied, and comparable successional stages may differ depending on regional environmental conditions. Whether these environmental differences influence the biomechanical properties of dune vegetation remains an open question, highlighting the need for site-specific assessments when integrating vegetation traits into coastal studies.

By addressing the following research questions, this study aims to fill the aforementioned knowledge gaps by providing a comprehensive biomechanical characterization of marram grass. This serves as a basis for improving vegetation modeling in experiments and contributes to a better understanding of dune vegetation dynamics, ultimately supporting the development of effective nature-based coastal protection strategies:

1. Are there significant seasonal variations in the biomechanical properties of dune vegetation that must be considered separately when modeling accretion processes (summer) and erosion processes (winter)?

2. Do different plant parts (sprouts, green leaves, brown leaves, flower stems) exhibit distinct biomechanical properties, or can they be treated as equivalent in biomechanical dune vegetation models?

3. Does wind exposure (e.g., windward vs. leeward sides of dunes) or geographical exposition (e.g., north-west vs. south-east) affect the biomechanical traits of vegetation, and if so, how should these factors be considered in biomechanical modeling?

4. How do biomechanical properties differ between vegetation in fixed, established dune systems and more dynamic dune systems, and how does this variation influence the accuracy and transferability of surrogate models for dune vegetation?

2 Methods

2.1 Study area

Field measurements were conducted on the East Frisian island Spiekeroog, which belongs to the North Sea barrier islands in Germany (see Figure 1a-b). The chain of barrier islands extends from Texel, the Netherlands to Fanø, Denmark, forming a landscape shaped by the littoral transport band driven by the counter-clockwise rotation of the tides into elongated west-east forms, further detailed by the interactions of waves, currents and wind (Pott, 1995). Located parallel to the coast, they isolate significant portions of the Wadden Sea from the open North Sea. From a geological perspective, these islands are very young, approximately 2000 years old, and were formed by an accumulation of Holocene marine sediments on a Pleistocene bed (Döring et al., 2021; Pollmann et al., 2018). By relocation of sandy sediments, pioneer dunes formed on the barrier islands and further evolved to dune chains reaching elevations of more than 20 metres above sea level (Pott, 1995). The side of the dune chains averted from the ocean, the backbarrier, is protected from high-energy wave action of the open sea and, moreover, is dominated by mild sedimentation conditions, allowing accumulation of fine-grained marine sediments and the development of salt marshes (Bakker, 2014; Pollmann et al., 2018). The geomorphology of the North Sea barrier islands is characterized by the predominance of sands, a low-lying coastal region and high storm tide frequency (Pott, 1995). The wind conditions at Spiekeroog and the whole German North Sea are dominated by westerly winds, but in general wind directions are substantially fluctuating in this area (Hild et al., 1999; Röper et al., 2013; Deutscher Wetterdienst). Due to human activities, e.g., dredging, land reclamation, and a resulting alteration of the sand sedimentation processes, North Sea barrier islands are characterized by sand accumulation and a resulting narrow pointed island tip in the East. As a result, the geomorphology of the western and the younger eastern area of the barrier islands differ (Röper et al., 2013; Pollmann et al., 2018). Spiekeroog is located in 5 km distance from the German mainland and is part of the national park "Niedersächsisches Wattenmeer". As a major objective, the German national parks enable undisturbed natural dynamics and landscape processes; to that end, entering dunes is mostly prohibited. The eastern part of the island, the locally called *Ostplate* (germ. *Ost* = East, germ. *-plate* = flat), is highly protected and developed eastwards between 1650 and 1960, so that Spiekeroog continuously grew several kilometers to its present East-West length of approx. 10 km (Röper et al., 2013). The older western area is characterized by a well-developed, fixed dune system consisting of white, gray and brown dunes lined up from the beach in the North towards the center of the island (Isermann and Cordes, 1997; Pollmann et al., 2018). These dune types differ significantly with regard to soil type and predominant vegetation species (Boorman, 1988; Davis, 2011; Röper et al., 2013). The white dunes of the Spiekeroog island are mainly covered by European beach grass or marram grass (*Calamagrostis arenaria*, formerly *Ammophila arenaria*) (Pott, 1995; Röper et al., 2013; Pollmann et al., 2018), which is native to the Atlantic coast of Europe, but due to worldwide planting for dune stabilization, it now colonizes dunes between 32°and 60°latitude on both sides of the equator (Pickart, 2021).

We conducted dune surveys at two white dune sites on Spiekeroog island (Fig 1b-d). The first site, referred to as Dune Ridge, is a 20 m wide strip of a dune chain located at the southwestern shore of the island ($53.753460° N, 7.674701° E$) and is part of the fixed dune system of Spiekeroog Island (Isermann and Cordes, 1997). The second site, termed Cusp Dune, is a freestanding dune situated at the northern beach near the transition to the *Ostplate* ($53.778793° N, 7.725181° E$), surrounded by dune breaches, and characterized by younger and mobile dune systems (Isermann and Cordes, 1997).

These two sites have been selected due to their distinct environmental conditions. The Dune Ridge site is located in an area prone to erosion, necessitating regular reinforcement measures, and characterized by more narrow beaches. Approximately 800 m north of the Dune Ridge, significant sand nourishments are periodically required to maintain the beach-dune system, with the most recent effort involving $80,000\,\mathrm{m}^3$ of sand in 2023 (NLWKN, 14.07.2023). In contrast, the Cusp Dune is part of a more dynamic system, situated at the edge of the *Ostplate*, which is characterized by wide beaches, young morphological changes, and is influenced by the west-to-east sediment drift typical for the North Frisian islands. Being a freestanding dune, the Cusp Dune is surrounded by water during storm surges and thus exposed to both erosion and accretion processes. Erosion taking place mainly along the luv side facing the North Sea and sedimentation along its flanks along the blow outs

Distinct study areas were established at each site based on dune morphology and wind exposure to investigate the impact on biomechanical vegetation traits. The Dune Ridge site (Fig. 2) was divided into three zones based on wind exposure: luv-side (sea-facing side, $160\,m^2$), dune crest ($135\,m^2$), lee-side (land-facing side, $240\,m^2$). The Cusp Dune site (Fig. 3) was segmented by geographical exposition into four zones: North (N, $550\,m^2$), East (E, $1490\,m^2$), West (W, $1497.5\,m^2$), and South (S, $350.5\,m^2$). The dune toe was extracted from DEM data using a 5° slope as delineation filter for both sites.

2.2 Field data collection

Field data was acquired monthly from January 2022 to December 2022 at the two dune sites. The data collection focused on (1) environmental parameters, (2) canopy height and horizontal density, and (3) plant sampling for laboratory analysis.

Environmental parameters

Detailed measurements of environmental parameters, including soil temperatures via soil sensors at both dune sites (see Figures 2 and 3), air temperature and precipitation, as well as wind forces, were collected. Furthermore, digital elevation models

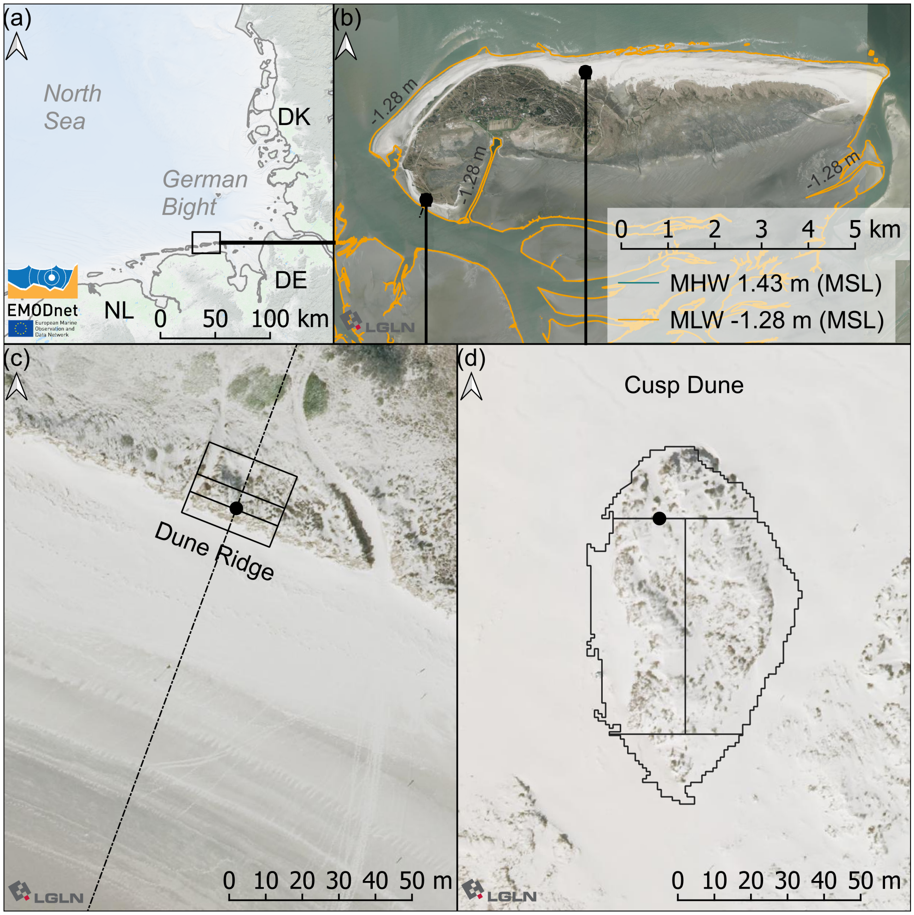

Figure 1. (a) Map of the German Bight with the focus area location. Based on EMODnet https://emodnet.ec.europa.eu/en/bathymetry. (b) Tidal barrier island Spiekeroog with tidal high and low water contour based on gauge data (GDWS, 2024) and DEM (NLWKN, 2023) and the two dune locations marked. (c) DuneRidge site and (d) Cusp Dune site - based on digital elevation model data (DEM) by Landesamt für Geoinformationen und Landesvermessung Niedersachsen (LGLN, engl.: State agency for geoinformation and state survey of Lower Saxony) data (LGLN, 2024). Mean high water (MHW) and mean low water (MLW) are extracted from the DEM using gauge related tidal water levels.

were evaluated. These data, along with methodological details and further findings, are provided in the Appendix (Sect. C).

Canopy height and horizontal density

Canopy height and horizontal density (see also Figures A1a-b, Sect. B1 in the Appendix) were measured in different quantities depending on the zone and dune site. For the Dune Ridge site, which consists of three zones (luv-side, dune crest, and lee-side), 20 measurements were taken in both the luv-side and lee-side zones, and 10 measurements at the dune crest per month. For the Cusp Dune site, which consists of four zones (North, East, South, West), 20 measurements were taken in both the North and

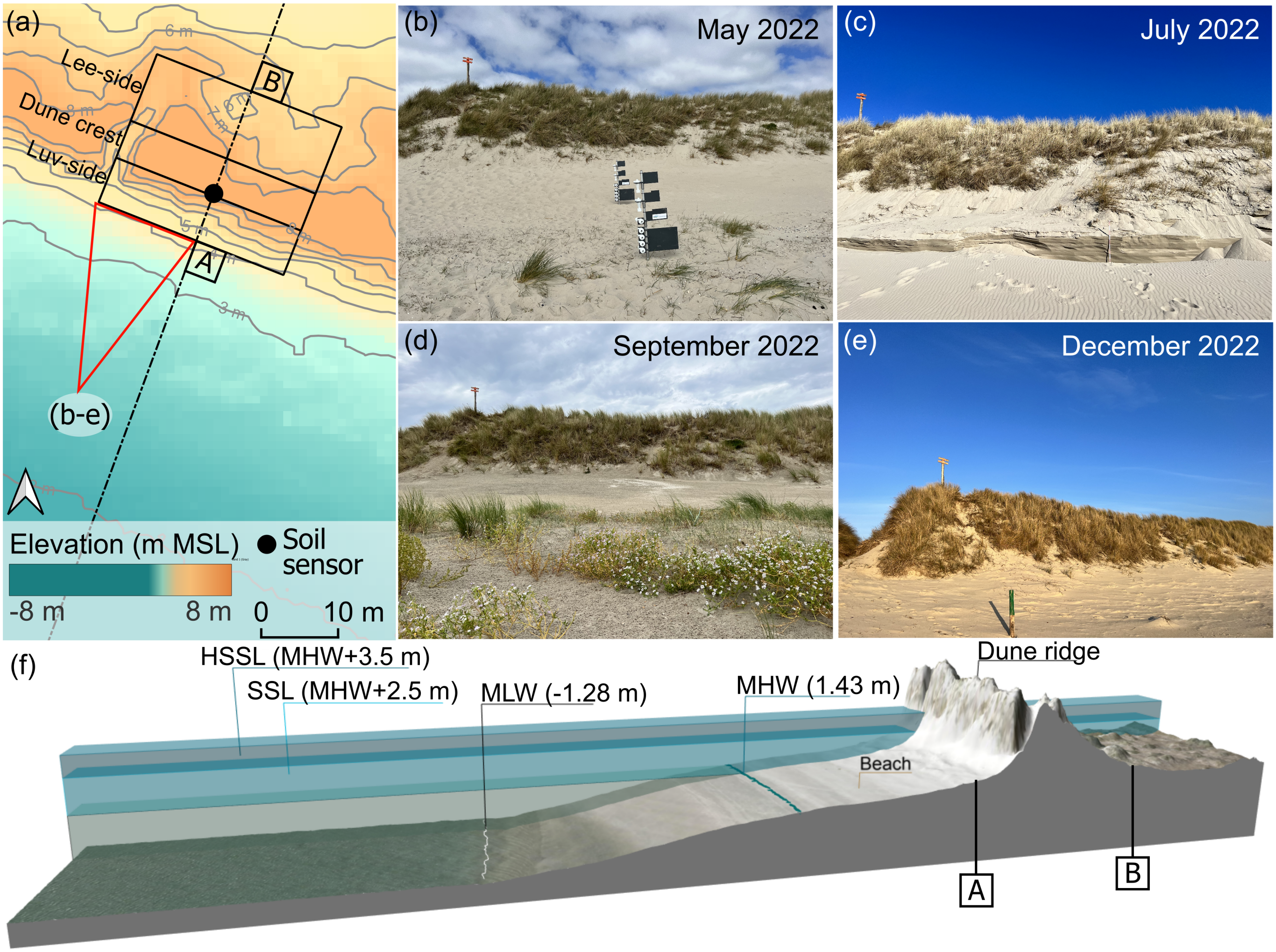

Figure 2. (a) Dune Ridge sectors with elevation based on a 2022 DEM (NLWKN, 2023), and positioning of the soil sensor. (b-e) View of the luv-side of the dune at different months. (f) Cross shore profile based on 2022 DEM, vertically superelevated by a factor of 3. For details on soil sensor information see Appendix C.

South zones, and 30 measurements in the East and West zones per month. Height measurements, referred to as canopy height, were conducted with a ruler with an accuracy of 1 mm. Canopy height was determined as the mean of random measurements representing the lower and upper boundaries of the canopy. Horizontal density was assessed using a metal frame with an internal area of 20 cmx20 cm. The number of individual shoots within the frame was manually counted to determine the horizontal density. During the flowering season, the number of flowers was also counted within the same area but recorded separately. These values were later extrapolated to one square meter. Measurements were taken at random locations with vegetation cover to equally represent dense and sparse areas. All measurements were consistently conducted by the same individual to minimize

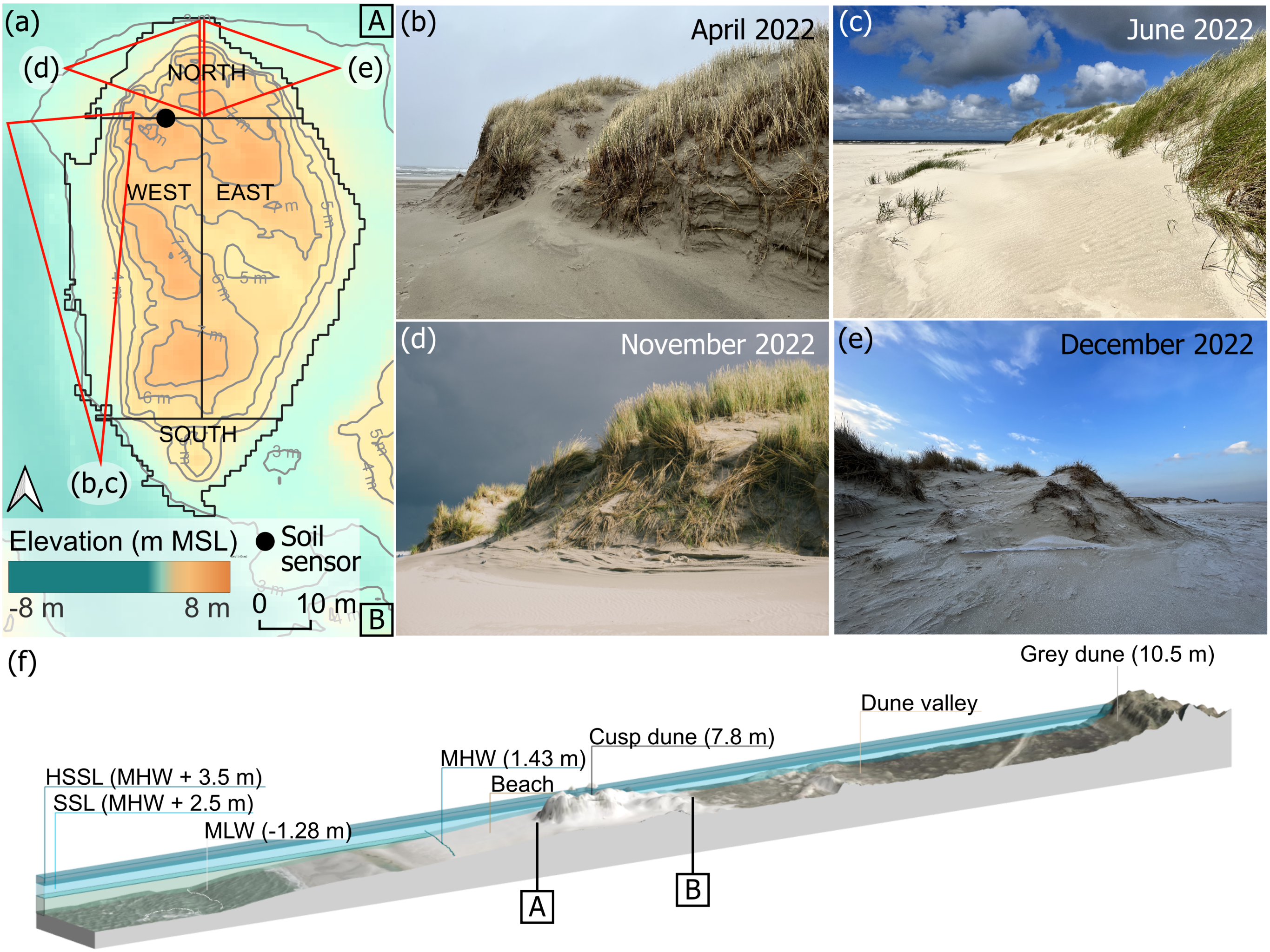

Figure 3. (a) Cusp Dune outline and sectors with elevation based on a 2022 DEM (NLWKN, 2023), and positioning of the soil sensor. (b) View of the western slope of the dune in April and (c) in June. (d) View of the north-western edge in November and (e) view of the north-eastern edge in December. View angles are indicated on (a) in red. (f) Cross shore profile based on 2022 DEM. For details on soil sensor information see Appendix C.

observer bias.

Plant sampling

Plant sampling focused on the dominant species, marram grass. For the Dune Ridge site, 20 samples were taken from both the luv-side and lee-side zones, and 10 samples from the dune crest zone per month for further laboratory analysis (e.g., three-point bending tests). For the Cusp Dune site, 20 samples were collected from both the North and South zones, and 30 samples from the East and West zones per month. Individual shoots and, during the flowering season, an additional three flower stems (hereafter referred to as stems) per zone and month were cut at ground level using garden scissors. The cut was angled towards the west using a digital compass, leaving a point at the sample bottom pointing west. This method ensured that the orientation of the plant in the field could be tracked in the laboratory, maintaining consistent loading direction during biomechanical tests, which might be influenced by wind exposure (see also Sect. A1 in the Appendix).

2.3 Laboratory analysis

The laboratory analysis involved dividing the collected samples into their individual structural components and conducting three-point bending tests to assess their biomechanical properties

Sample preparation and plant parts

The sampled shoots of marram grass were divided into three main structural components: sprout, green leaf, and brown leaf. The sprout was defined as the lower part of the shoot up to the first branching leaf. In the laboratory, the sprout was separated from the shoot by cutting at this point. Leaves were also separated at their point of branching from the shoot. During the flowering season, stems, including the flower, were also collected and treated as a separate component, thus not requiring cutting (see also Sect. A1 in the Appendix).

For each zone and month, ten sprouts, three green leaves, three brown leaves, and, if applicable, three stems were analyzed. The samples were processed and tested within 1-2 days; prior to processing, they were stored upright in a vase-like container with a small amount of water to prevent wilting.

Measurement of length and outer diameter

The length (L) and outer diameter (d_o) of each plant part were important geometric parameters for biomechanical analysis. Lengths were measured in centimeters using a tape measure with an accuracy of 1 mm, though the practical reading accuracy may be lower. The outer diameter was measured at the location where the three-point bending tests were to be conducted: at half the length ($L/2$) for sprouts and stems, and at one-third the length ($L/3$) for leaves (see also Sect. B1 in the Appendix). These diameters were measured using a digital caliper with a resolution of 0.01 mm.

Three-point bending tests

The three-point bending tests were performed according to ISO 178 (2019). Each plant part was cut into 6 cm long sections, with the measurement point of the outer diameter d_o located at the midpoint of these sections.

The bending tests utilized a universal testing machine, the „zwickiLine Z0.5“ by ZwickRoell GmbH & Co.KG. This machine was equipped with a load cell, calibrated in compliance with DIN EN ISO 7500-1 (2018), ranging from 0.2 N to 50 N. The displacement measurement had an uncertainty of 0.0830 m. The loading edges and supports had radii of 5 mm, and the span between the supports (Δs) was 40 mm. The displacement rate was maintained at 0.05 mm/s, adhering to quasi-static deformation standards outlined by Liu et al. (2021). A preload of $0.05\,\mathrm{N}$ was applied to the samples before measurements commenced.

The bending tests produced force-deflection curves, which were essential for analyzing the mechanical properties of each sample. From these curves, the force (F) and deflection (D) were used to compute the bending stiffness (K_B = F/D, hereafter referred to as stiffness) and the Young's modulus E of each sample, calculated from the initial slope of the force-deflection curve. The Young's modulus, also known as the elastic modulus, quantifies the stiffness of a material and describes its resistance to deformation under an applied load. For plant components, it provides insight into their structural role, with a higher Young's modulus indicating stiffer materials that deform less under mechanical stress, enhancing stability, and a lower modulus reflecting greater flexibility, enabling reconfiguration to reduce mechanical damage. In this study, the experimental determination of Young's modulus includes the geometry of the plant components through the second moment of area (I), which assumes a solid circular cross-section based on the outer diameter (d_o) of the sample:

$$I = \frac{\pi (d_o)^4}{64} \tag{1}$$

The following equation was used to calculate the Young's modulus:

$$E = \frac{4(s)^3 F}{3D\pi (d_o)^4} \tag{2}$$

In this study, the deflection range selected was between $0.4\,\mathrm{mm}$ and $1.2\,\mathrm{mm}$, based on the initial linear portion of the force-deflection curve observed across all samples.

The flexural stiffness (EI) was then calculated by multiplying Young's modulus (E) by the second moment of inertia (I).

The maximum force ($F_{\max}$), also referred to as the breaking force, was determined as the peak value on the force-deflection curves (Zhu et al., 2020; Liu et al., 2021). For marram grass, failure is more accurately characterized by folding rather than breaking. The flexural strength was then calculated using the equation:

$$\sigma = \frac{40 d_o F_{\max}}{8I} \tag{3}$$

The results from the bending tests provide a valuable data set (Kosmalla et al., 2024) of the plant components, such as Young's modulus (E), stiffness (K_B), flexural stiffness (EI), and flexural strength (). These parameters are vital for understanding the mechanical behavior of marram grass, which plays a crucial role in the resilience and adaptation of dune ecosystems. In particular, Youngs modulus (E) reflects the material stiffness of plant tissues, determining their ability to withstand mechanical stress, with higher E values indicating increased resistance to bending and deformation under waves, wind and sediment transport forces. Previous studies have shown that plant stiffness is a key factor in counteracting mechanical forces in coastal environments (Bouma et al., 2005; Paul et al., 2016), highlighting its potential role in dune stabilization.

2.4 Data analysis

To streamline the data analysis process and enhance the interpretation of the results, the monthly data were aggregated into seasonal intervals. The seasons were defined as "summer" (April to September) and "winter" (October to March). This categorization reflects the primary dune dynamics: erosion processes, which predominantly occur in winter, and accretion processes, which mainly happen in summer (Pye and Blott, 2016). This differentiation aims to capture potential seasonal variations in the biomechanical properties of marram grass, relevant for experimental modeling of natural dune dynamics. An exception to this seasonal aggregation was made for the analysis of wind influence and dune site comparisons, where year-round data were considered.

For the analysis of biomechanical properties, the data from both dune sites were aggregated. This includes parameters such as canopy height, horizontal density, number of flowers, and the biomechanically relevant properties of the individual plant components (sprout, green/brown leaf, stem): Length, outer diameter, stiffness, and Young's modulus. Exceptions include the investigation of wind influence, where data from the Dune Ridge were compared between the windward (luv) and leeward (lee) sides. For the Cusp Dune, the zones were aggregated into Northwest (North and West) and Southeast (South and East). This approach for the Dune Ridge is based on the assumption that the landward side is more sheltered from the wind, while for the Cusp Dune, it is more directly based on the actual wind conditions during the study year. For the comparison between dune sites, the data for each site were aggregated across all months and zones. Given that our data were not normally distributed, the nonparametric Mann-Whitney test was employed to assess the significance of observed differences among our samples. The Mann-Whitney statistics tests for differences between two groups on a single, ordinal variable without assuming a specific distribution of the data (Bauer, 1972).

In total, 1543 sprout samples (Dune Ridge: 491, Cusp Dune: 1052), 831 green leaf samples (Dune Ridge: 227, Cusp Dune: 614), and 823 brown leaf samples (Dune Ridge: 224, Cusp Dune: 599), and 389 stem samples (Dune Ridge: 115, Cusp Dune: 274) were investigated. The aggregated data were analyzed using Mann-Whitney U tests to statistically examine the following comparisons:

1. Biomechanical differences between plant parts: The biomechanical parameters (K_B, E, d_o, L) of sprouts, green leaves, brown leaves, and stems were compared seasonally to determine whether different plant parts exhibit distinct biomechanical properties. This analysis aggregated data from both dune sites.

2. Seasonal variations: The biomechanical parameters (K_B, E, d_o, L) of each plant part were compared between the "summer" (April to September, relevant for accretion processes) and "winter" seasons (October to March, relevant for erosion processes) to detect any significant seasonal variations in the biomechanical properties of the dune vegetation. This analysis aggregated data from both dune sites.

3. Impact of wind exposure and geographical exposition: The biomechanical parameters (K_B, E, d_o, L) of each plant part were compared for the Dune Ridge site between windward (luv-side) and leeward (lee-side) zones, and for the Cusp Dune

site between Northwest and Southeast zones to evaluate the influence of wind exposure and geographical exposition on biomechanical traits.

4. Differences between dune systems: The biomechanical parameters (K_B, E, d_o, L) of each plant part from the Dune Ridge (fixed, established dune system) and Cusp Dune (more dynamic dune system) sites were compared. For each plant component, data from the entire site, aggregated across all months and zones, were compared between the two dune systems to investigate how biomechanical properties differ between these two types of dune systems.

3 Results

3.1 Seasonal variations in biomechanical properties of marram grass

3.1.1 Geometric characteristics

Canopy height, horizontal density, and number of flowers

Canopy height (Fig. 4a) showed no significant difference between summer (79.66 ± 15.62 cm) and winter (79.87 ± 13.38 cm) measurements ($p = 0.3429$). Horizontal density (Fig. 4b), however, was significantly higher in summer (493.49 ± 217.97 shoots per mš) compared to winter (445.65 ± 209.93 shoots per mš, $p < 0.001$). The number of flowers (Fig. 4c), observed only in summer, was on average 108.86 ± 92.50 flowers per mš. The results of the statistical analysis are provided in the Appendix (Sect. D, Table D1).

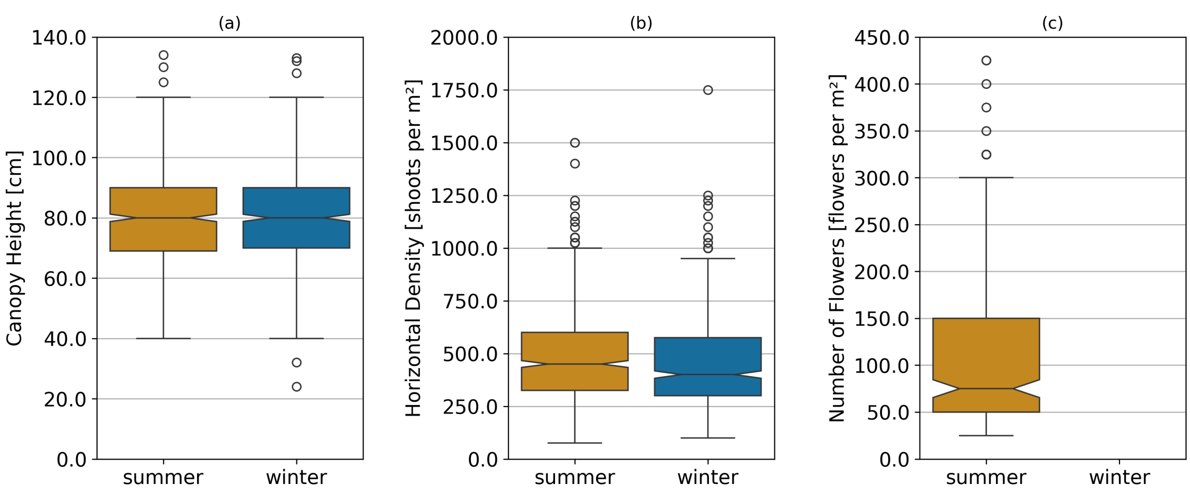

Figure 4. Combined data from both dune sites showing (a) Canopy height in cm, (b) Horizontal density in shoots per m, and (c) Number of flowers in flowers per m, comparing summer and winter illustrated as boxplots. Note that no flowering was observed in winter, and thus not corresponding bar is shown for this season in (c).

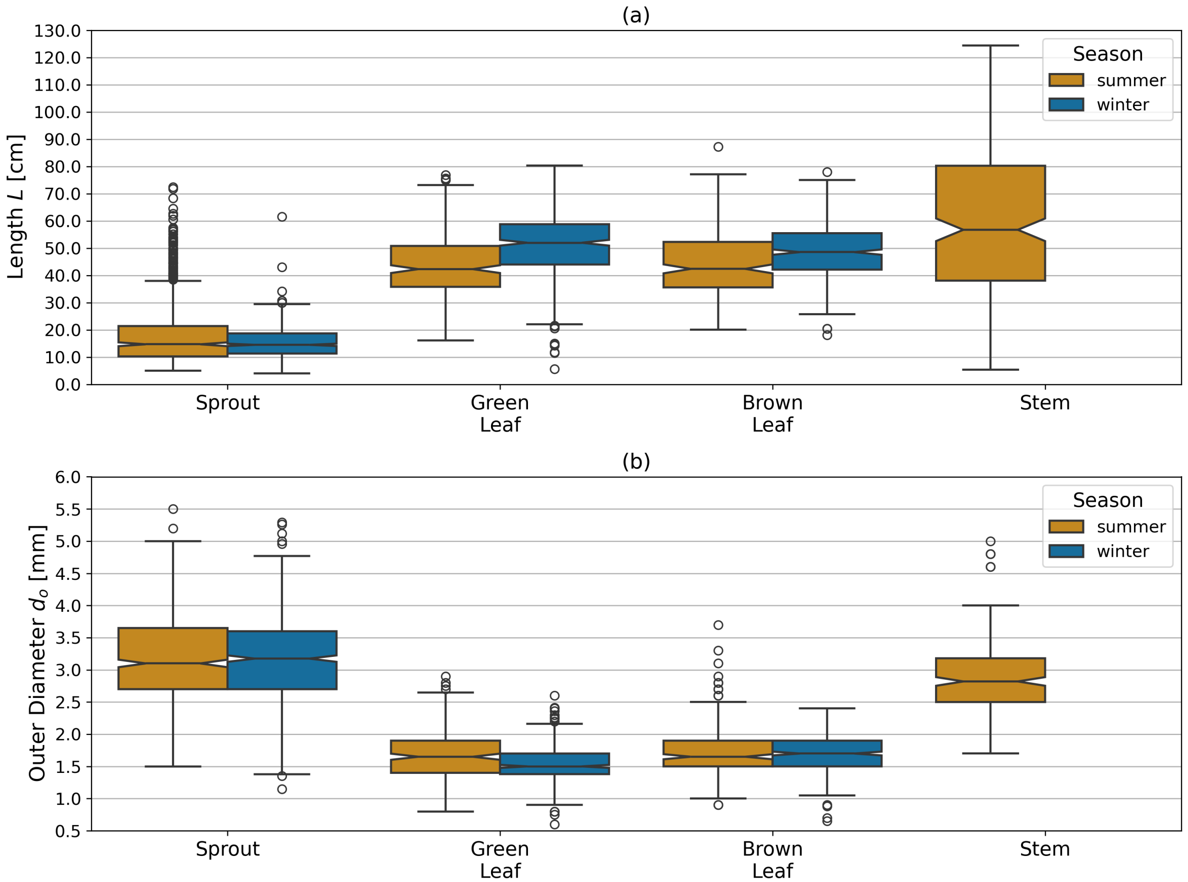

Figure 5. Combined data from both dune sites showing (a) mean length L and (b) mean outer diameter d_o of plant components (sprout, green leaf, brown leaf, stem) comparing summer and winter illustrated as boxplots. Note that no stems were observed in winter.

Length and outer diameter of plant components

The seasonal length and outer diameter of plant components are shown in Fig. 5a and b, respectively. Sprouts showed no significant seasonal variation in length between summer (18.28 ± 5.11 cm) and winter (15.37 ± 4.45 cm, $p = 0.196$). The outer diameter of sprouts also remained consistent across seasons (summer: 3.24 ± 0.53 mm, winter: 3.10 ± 0.51 mm, $p = 0.909$). Green leaves exhibited a significant increase in length during winter (51.47 ± 8.94 cm) compared to summer (44.35 ± 8.14 cm, $p < 0.001$). The outer diameter of green leaves was significantly larger in summer (1.69 ± 0.22 mm) than in winter (1.57 ± 0.20 mm, $p < 0.001$). For brown leaves, the length increased significantly from summer (43.80 ± 6.93 cm) to winter (47.82 ± 7.95 cm, $p < 0.001$). The outer diameter of brown leaves did not show significant seasonal variation between summer (1.72 ± 0.26 mm) and winter (1.67 ± 0.21 mm, $p = 0.199$) measurements. The length and outer diameter of stems were consistently measured in summer only, showing on average a length of 64.94 ± 10.87 cm and an outer diameter of 2.78 ± 0.39 mm. The results of the statistical analysis are provided in the Appendix (Sect. D, Tables D2 and D3).

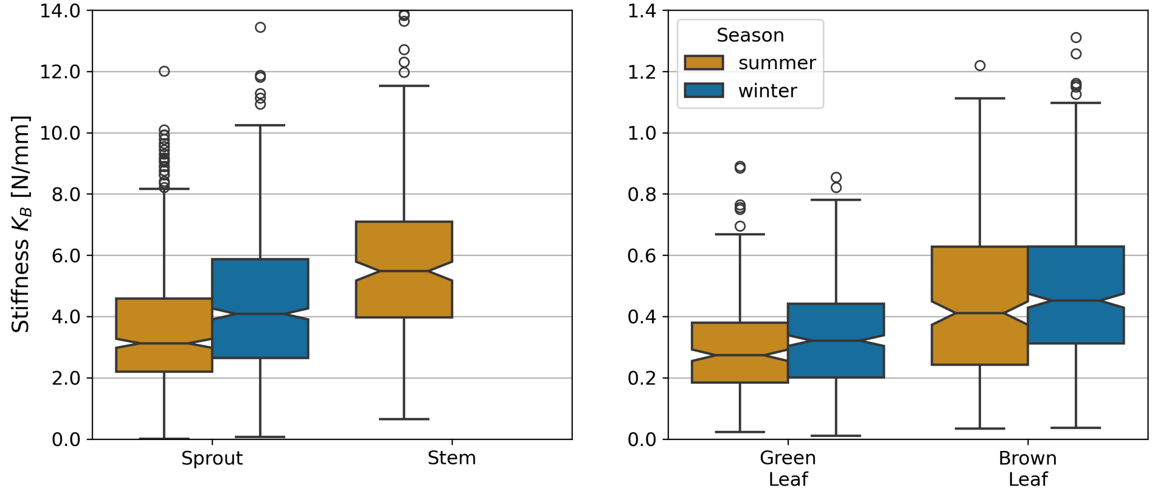

Figure 6. Stiffness K_B of each plant component in summer and winter months, based on combined data from both dune sites. 18 outlier values for brown leaves and 1 for stems were excluded for visual clarity. Note that no stems were observed in winter.

3.1.2 Mechanical characteristics

Stiffness

Stiffness showed significant seasonal variations in some plant components. To highlight the similarities between sprout and stems, these components are displayed together, while green and brown leaves, which exhibit distinct stiffness patterns, are presented in a seperate plot (Fig. 6). For sprouts, stiffness was significantly higher in winter (4.15 ± 1.59 N/mm) compared to summer (3.98 ± 1.46 N/mm, $p < 0.001$). Green leaves also exhibited a significant seasonal difference, with higher stiffness in winter (0.33 ± 0.13 N/mm) than in summer (0.29 ± 0.11 N/mm, $p = 0.001$). Brown leaves showed no significant seasonal variation in stiffness (0.70 ± 0.46 N/mm in summer and 0.47 ± 0.18 N/mm in winter, $p = 0.077$). Stems were only measured in summer, with a mean stiffness of 5.30 ± 1.65 N/mm. The results of the statistical analysis are provided in the Appendix (Sect. D, Tables D2 and D3).

Young's modulus

Young's modulus displayed notable seasonal variations for certain plant components (Fig. 7). For sprouts, Young's modulus was significantly higher in winter 1173.47 ± 479.92 MPa) compared to summer (1175.85 ± 563.72 MPa, $p < 0.001$). Green leaves also exhibited considerable seasonal differences, with Young's modulus being greater in winter (1585.21 ± 624.35 MPa) than in summer (1215.16 ± 526.92 MPa, $p < 0.001$). In contrast, brown leaves did not show significant seasonal variations in Young's modulus (1790.77 ± 809.09 MPa during summer and 1837.46 ± 855.73 MPa in winter, $p = 0.898$). Measurements for stems were only taken in summer, with a mean Young's modulus of 2641.05 ± 1152.78 MPa. The results of the statistical analysis are provided in the Appendix (Sect. D, Tables D2 and D3).

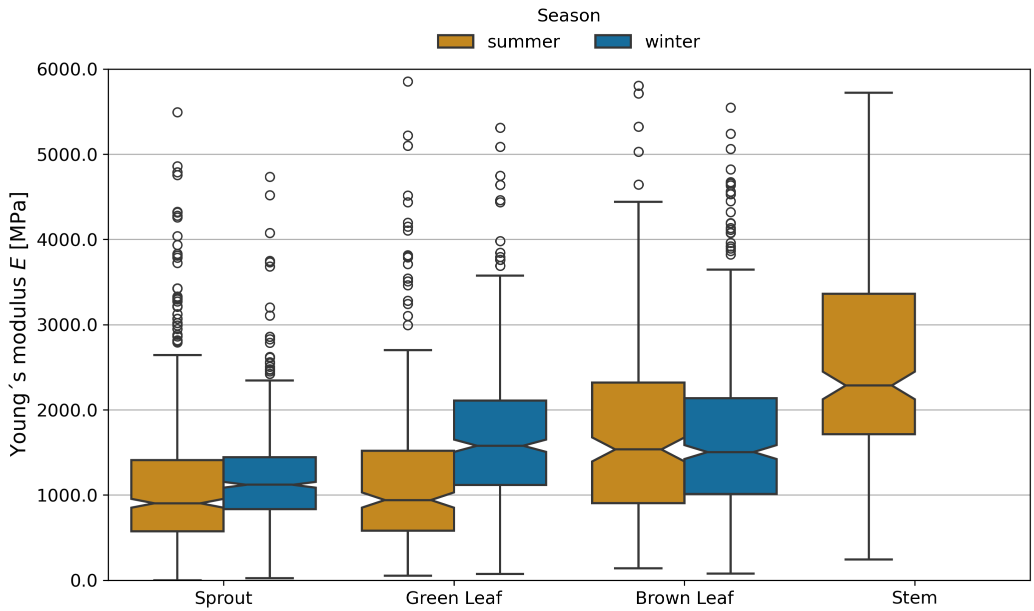

Figure 7. Young's modulus E of each plant component in summer and winter months, based on combined data from both dune sites. One outlier value for sprouts, four for green leaves, nine for brown leaves, and five for stems were excluded for visual clarity. Note that no stems were observed in winter.

3.2 Comparison of biomechanical traits among plant parts

Significant differences in the biomechanical parameters stiffness (K_B), Young's modulus (E), outer diameter (d_o), and length (L) were found between all plant components (sprout, green leaf, brown leaf, stems) in both summer and winter (all $p < 0.001$), with the exception of Young's modulus between sprouts and green leaves in summer ($p = 0.319$), Young's modulus between green and brown leaves in winter ($p = 0.399$), and the outer diameter and length between green and brown leaves in summer ($p = 0.830$ and $p = 0.611$, respectively).

For stiffness (Fig. 6), all plant parts exhibited significant differences. In summer, stems had the highest stiffness values, followed by sprouts, brown leaves, and green leaves. During winter, the pattern remained consistent, excluding stems. In terms of the Young's modulus (Fig. 7), stems exhibited significantly higher values compared to other plant parts in summer. Brown leaves, green leaves, and sprouts followed. This order persisted in winter, excluding stems. Notably, there were no significant differences between sprouts and green leaves in summer, and between green and brown leaves in winter. For length (Fig. 5a), stems were significantly longer than the other parts in summer, with green leaves, brown leaves, and sprouts following. This trend remained in winter, excluding stems. In summer, no significant difference was found between green and brown leaves. Regarding outer diameter (Fig. 5b), sprouts had the significantly largest diameters in summer, followed by stems, brown leaves, and green leaves. In winter, the pattern remained consistent, excluding stems. The only exception was between green and brown leaves in winter, where the difference was not significant. The results of the statistical analysis are also provided in the Appendix (Sect. D, Table D4).

3.3 Impact of wind exposure on biomechanical traits

Stems exhibited no significant differences in any of the measured parameters (K_B, E, d_o, and L) between luv and lee-side or the Northwest and Southeast sides, respectively.

For Dune Ridge (Fig. 8-10), the stiffness and Young's modulus of sprouts were significantly greater on the lee-side (4.40 ± 1.92 N/mm and 1374.14 ± 708.41 MPa) compared to the luv-side (3.31 ± 1.82 N/mm and 1048.84 ± 796.39 MPa, $p < 0.001$ for both parameters). Green leaves exhibited significantly greater stiffness (0.35 ± 0.17 N/mm), Young's modulus (1910.30 ± 1094.54 MPa), and length (52.44 ± 12.27 cm) on the lee-side compared to the luv-side (0.28 ± 0.15 N/mm, 1423.17 ± 842.79 MPa, and 44.92 ± 10.13 cm) with p-values of 0.010, 0.002, and < 0.001 respectively. Brown leaves showed no significant differences in stiffness, Young's modulus, and outer diameter between the luv and lee-side. However, the length of brown leaves was significantly greater on the lee-side (48.62 ± 11.87 cm) compared to the luv-side (43.28 ± 10.13 cm, $p = 0.003$).

Overall, all found trends at Dune Ridge indicate that the values of the respective parameters are significantly greater on the lee-side than on the luv-side.

For Cusp Dune (Fig. 8-10), the Young's modulus (1162.39 ± 693.30 MPa) and length (17.20 ± 8.32 cm) of sprouts were significantly greater on the Northwest side compared to the Southeast side (1069.36 ± 637.48 MPa and 16.51 ± 9.51 cm with p-values of 0.020 and 0.015 respectively). Green leaves showed no significant differences in stiffness, Young's modulus, and length between the Northwest and Southeast sides. However, the outer diameter of green leaves was significantly greater on the Southeast side (1.63 ± 0.34 mm) compared to the Northwest side (1.57 ± 0.31 mm, $p = 0.030$). Brown leaves exhibited significantly greater stiffness (0.60 ± 0.81 N/mm) and Young's modulus (1686.62 ± 1041.84 MPa) on the Northwest side compared to the Southeast side (0.47 ± 0.51 N/mm and 1581.99 ± 1450.23 MPa, $p = 0.002$ and $p = 0.015$ respectively). While there is a tendency for the parameters stiffness, Young's modulus, and length to be greater in the Northwest, the outer diameter tends to be larger in the Southeast.

At both dune sites, the most significant differences were observed in the parameter Young's modulus, followed by stiffness and length, with the outer diameter showing the weakest differences.

3.4 Influence of dune systems on plant biomechanics

In comparing the biomechanical traits between the two dune systems, Dune Ridge and Cusp Dune, several significant differences were observed. Stems exhibited no significant differences in any of the measured parameters (K_B, E, d_o, and L) between Dune Ridge and Cusp Dune, indicating similar mechanical behavior across these systems for this plant part.

For sprouts, the Young's modulus was significantly higher at Dune Ridge (1243.01 ± 816.02 MPa) compared to Cusp Dune (1115.39 ± 666.96 MPa, $p = 0.002$). The outer diameter was significantly larger at Cusp Dune (3.20 ± 0.73 mm) com-

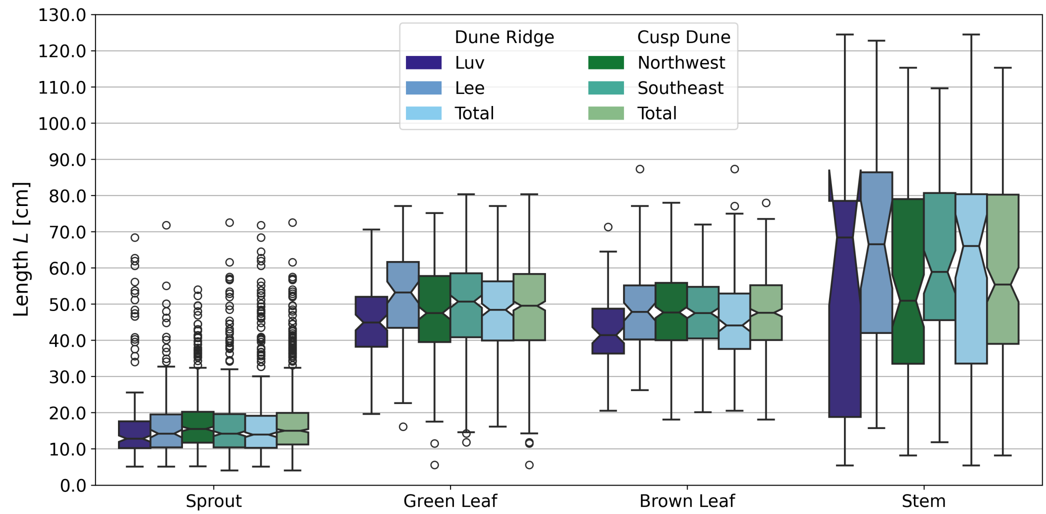

Figure 8. Comparison of luv-side and lee-side at Dune Ridge as well as Northwest-side and Southeast-side at Cusp Dune with boxplots showing length L for each plant part, based on year-round data.

pared to Dune Ridge (3.11 ± 0.63 mm, $p = 0.043$). Additionally, the length of sprouts was slightly greater at Dune Ridge (16.99 ± 11.23 cm) compared to Cusp Dune (16.85 ± 8.94 cm, $p = 0.039$).

Green leaves showed a significantly higher Young's modulus at Dune Ridge (1647.10 ± 1021.48 MPa) compared to Cusp Dune (1475.76 ± 972.71 MPa, $p = 0.031$). However, there were no significant differences in stiffness, outer diameter, and length.

Brown leaves exhibited the most pronounced differences between the two dune systems. The Young's modulus was significantly higher at Dune Ridge (2159.01 ± 1425.67 MPa) compared to Cusp Dune (1634.93 ± 1260.05 MPa, $p < 0.001$), and the stiffness was also greater at Dune Ridge (0.63 ± 0.79 N/mm) compared to Cusp Dune (0.54 ± 0.68 N/mm, $p = 0.036$). The outer diameter of brown leaves was significantly larger at Cusp Dune (1.72 ± 0.30 mm) compared to Dune Ridge (1.65 ± 0.33 mm, $p < 0.001$). The length of brown leaves was also significantly greater at Cusp Dune (47.35 ± 10.34 cm) compared to Dune Ridge (45.61 ± 11.34 cm, $p = 0.010$).

Overall, the Young's modulus was consistently higher at Dune Ridge across all plant parts except for stems. The outer diameter tended to be larger at Cusp Dune, particularly for sprouts and brown leaves. Length did not show a clear trend, with significant differences observed only for sprouts and brown leaves. Stiffness differences were primarily notable in brown leaves, with higher values at Dune Ridge.

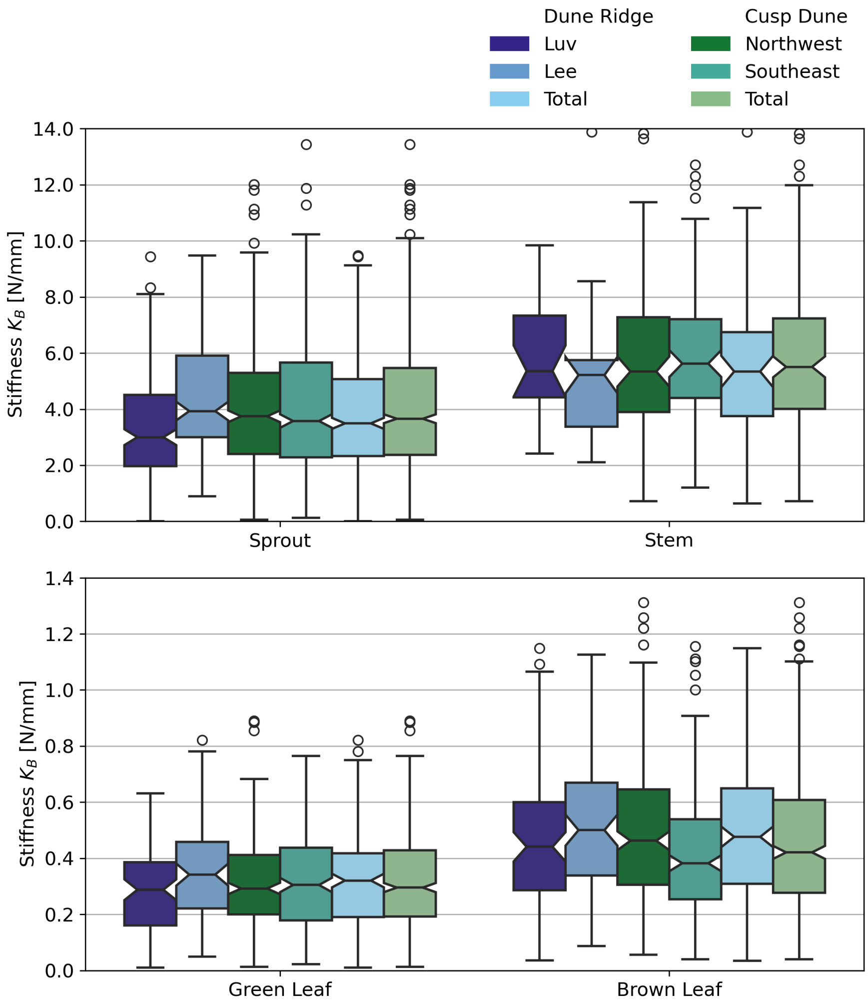

Figure 9. Comparison of luv-side and lee-side at Dune Ridge with boxplots showing stiffness K_B for each plant component, based on year-round data. To improve clarity, sprouts and stems are grouped together due to their similar mechanical characteristics, while green and brown leaves are shown separately to emphasize their distinct behavior. Note that 33 outlier values for brown leaves, and 2 for stems were excluded for visual clarity.

4 Discussion

This study aims to provide detailed biomechanical parameters of marram grass to facilitate advanced modeling of dune vegetation. Current models often simplify or ignore traits in flexible vegetation, using surrogates like wooden dowels (e.g., Kobayashi et al. (2013); Bryant et al. (2019)), which do not accurately reflect the dynamic interactions between vegetation and dune environments. Our analysis incorporates the seasonality of dune dynamics, with accretion processes in summer and erosion processes in winter, as well as the growth cycles of the vegetation. This approach enables a more realistic simulation of the

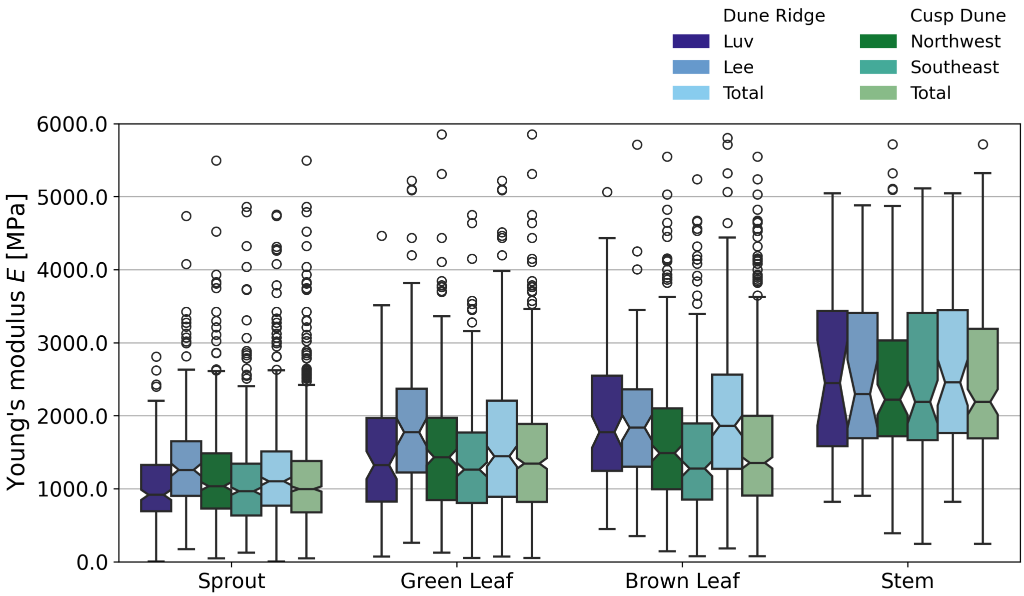

Figure 10. Comparison of luv-side and lee-side at Dune Ridge as well as Northwest-side and Southeast-side at Cusp Dune with boxplots showing Young's modulus E for each plant component, based on year-round data. Note that 2 outlier values for sprouts, 8 for green leaves, 17 for brown leaves, and 10 for stems were excluded for visual clarity.

role of vegetation in dune stabilization and coastal defense strategies. Additionally, our findings underscore the relevance of biomechanical diversity among plant parts for improving the fidelity of dune models. In the following sections, we discuss our findings in detail, exploring the implications for improving the accuracy of dune vegetation models.

4.1 Seasonal variations in biomechanical traits

Understanding seasonal variations in plant properties is crucial for surrogate modeling because both dune dynamics and plant traits are subject to significant seasonal changes. Similar to findings on salt marsh vegetation, our results show that during summer, vegetation density significantly increases, while in winter, the stiffness of the vegetation is greater and the outer diameter smaller (Vuik et al., 2017; Foster-Martinez et al., 2018; Keimer et al., 2024; Li et al., 2024). Instead, our observations suggest that leaves, which lengthen in winter, may play a critical role in dune resistance to storm events, as they directly contribute to key factors highlighted by Feagin et al. (2015), such as leaf area, plant architecture, and aboveground biomass, which influence vegetation-wave in salt marshes. This dynamic adaptability of marram grass, with increased stiffness in winter for erosion resistance and greater density in summer to enhance accretion, supports the natural processes of dune formation and recovery, reinforcing the role of vegetation in maintaining dune resilience.

Canopy height showed no seasonal differences (annual average of 80 ± 15 cm), aligning with the growth range reported by Hesp (1981) and Bressolier and Thomas (1977).

Horizontal density was higher in summer, consistent with findings by Li et al. (2024) and Vuik et al. (2017), who noted increased vegetation density during the growth season. However, the density observed in this study was within the upper range of previous studies (Seabloom and Wiedemann, 1994; Zarnetske et al., 2012; Feagin et al., 2019). Our results showed that the number of flowers, observed only in summer, averaged 109 ± 93 flowers m^{-2}, which is significantly higher than the approximately 30 flowers m^{-2} reported by Seabloom and Wiedemann (1994). This seasonal occurrence of flowers must be taken into account in modeling efforts.

For sprouts, significant seasonal variations were observed in both stiffness and Young's modulus, with higher values in winter compared to summer.

Furthermore, higher Young's modulus values were found for the exposed North-Western tip of the Cusp Dune site, coinciding with the area showing the largest erosion of the site (see Figure C1a in the Appendix. Interestingly for the Dune Ridge site, larger Young's modulus values were measured along the sheltered lee side, showing accretion in the DEM analysis (see Figure C2a in the Appendix), compared to the exposed luv side. The sprout length measurements can be compared to the stem heights up to 195 mm reported by Feagin et al. (2019), highlighting the importance of precise definitions of plant parts in such studies. However, longer sprouts were measured for the exposed North-West tip of the Cusp Dune site, prone to erosion, compared to the South-West sector, which shows accretion. This might well coincide with morphological changes identified in the DEMs, meaning the erosion uncovers the sprouts at the northern edge, while the identified sedimentation buries them at the southern end (compare Figure C2a in the Appendix). Similarly, the sprout diameter aligns with the stem diameter of 3 ± 1 mm found by Feagin et al. (2019). Seasonal variations in sprout parameters were minor and can be averaged annually for modeling purposes.

For green leaves, significant seasonal differences were observed in length, stiffness, and outer diameter. Green leaves were longer in winter, likely due to older leaves persisting through the season, contrasting trends observed in salt marsh species (Li et al., 2024; Koch et al., 2009). Conversely, the outer diameter of green leaves was larger in summer, which aligns with the findings of Vuik et al. (2017). Larger green leaf diameters were found along the sheltered lee side of the Ridge Dune site, whilst longer green leaves were identified at the sheltered South-West area of the Cusp Dune site. These findings indicate, that the plants develop larger phenological aboveground canopy in wind sheltered areas compared to the exposed luv-oriented zones. However, the differences in stiffness and outer diameter between summer and winter were minor (summer: 0.29 ± 0.11 kN/m and 1.7 ± 0.2 mm; winter: 0.33 ± 0.13 kN/m and 1.6 ± 0.2 mm), making it practical to use an annual average for these parameters in modeling efforts, especially for physical models where replicating such minor variations may be challenging.

For brown leaves, the only seasonal difference observed was in length, with brown leaves also being longer in winter, while stiffness and outer diameter remained constant, allowing for their annual averaging.

For stems, specifically flower stems, the summer-only presence highlights their importance for models representing the summer state. Their significant contribution to overall plant density, height, and stiffness make them critical components in summer models where their structural contribution to accretion processes is essential.

Overall, stiffness exhibited seasonal variations for both sprouts and green leaves, with higher values in winter. This trend aligns with Vuik et al. (2017), who speculated that winter vegetation tends to be stiffer due to lower temperatures and the fracturing of less resilient parts. However, these differences are not substantial enough to significantly impact physical modeling, indicating that seasonal variations in these parameters are negligible for modeling purposes and thus can be averaged annually. However, the increased stiffness and Young's modulus in winter suggest that dune vegetation is more resistant to mechanical stress during this period, potentially enhancing dune stability. Conversely, the greater flexibility and density in summer indicate a higher capacity for growth and dune accretion processes. In summary, the significant seasonal variations in the biomechanical properties of marram grass highlight the need for seasonally adjusted modeling parameters in dune dynamics studies. Notably, three key aspects must be considered:

1. A major seasonal difference is the presence of flowers in summer, which must be accounted for in modeling.

2. The difference in horizontal density between seasons must be incorporated into surrogate models with an increased density in summer.

3. Besides flowers and density, only the length differences of the leaves are relevant and should be considered in modeling efforts.

4.2 Differentiation among plant parts

The variability in outer diameter and length among plant parts necessitates distinct consideration in modeling efforts. Sprouts and stems, with their larger diameters, offer robust resistance against physical forces. The differences in length, particularly the significant disparity between stems and other plant parts, further emphasize the need to account for each part's geometric characteristics to accurately represent their contributions to dune morphology. However, the lack of significant difference in outer diameter and length between green and brown leaves in summer, along with the relatively small differences in stiffness and length in winter, indicate that, for these parts, a simplified representation might be sufficient.

Given the close similarity between green and brown leaves, and considering the practicalities of physical modeling, where precise distinctions may not be easily implemented, the following simplified properties, averaged from green and brown leaves, can be applied for leaves in general:

– Summer: Length = $44 \pm 8\,\mathrm{cm}$, Outer Diameter = $1.7 \pm 0.2\,\mathrm{mm}$, Stiffness = $0.45 \pm 0.2\,\mathrm{kN/m}$

– Winter: Length = $50 \pm 9\,\mathrm{cm}$, Outer Diameter = $1.7 \pm 0.2\,\mathrm{mm}$, Stiffness = $0.45 \pm 0.2\,\mathrm{kN/m}$

The significant differences in stiffness and Young's modulus between plant parts also underscore the need to model each component separately. Stems, with their highest values for both parameters, provide the greatest structural support. In contrast, green and brown leaves, which showed lower stiffness and Young's modulus, contribute more to flexibility and dynamic responses to environmental forces.

Ignoring these differences could lead to inaccuracies in predicting vegetation behavior and its impact on dune dynamics, resulting in models that do not adequately reflect the true mechanical properties and structural roles of the vegetation, though in some cases, a simplified approach may still be appropriate without compromising model accuracy.

4.3 Impact of wind on plant biomechanics

The impact of wind exposure on the biomechanical traits of dune vegetation reveals significant variations between windward and leeward sides of the dunes, most notably in stiffness and Young's modulus. Stems exhibited no significant differences between wind-exposed and sheltered sides, indicating uniform structural response, while the greatest variations occurred in sprouts.

Significant differences in stiffness and Young's modulus between windward and leeward sides suggest these parameters are most sensitive to wind exposure and likewise to coupled aeolian sediment transport (see Figure C1a and C2a in the Appendix). At Dune Ridge, the leeward side exhibited greater stiffness and Young's modulus, which may indicate an avoidance strategy, where vegetation increases flexibility on the windward side to reduce wind impact. Conversely, at Cusp Dune, the more wind-exposed northwest zone showed higher stiffness and Young's modulus, suggesting a tolerance strategy with vegetation maximizing its resistance to breakage to withstand wind forces.

Wind data from 2022 showed predominantly west-dominated winds, with the highest frequency from the northwest during summer, while in winter, southwest winds were more prevalent, though the strongest winds (Bft 6) predominantly originated from northwest (see also Sect. C2 in the Appendix). As a result, the southwest-facing Dune Ridge coastline complicates wind exposure impact assessment, and comparisons between Northwest and Southeast zones showed few significant differences, suggesting no strong wind exposure effect on plant biomechanics. Consequently, wind influence will not be included in the biomechanical parameterization of marram grass.

4.4 Influence of dune type on plant biomechanics

Higher stem density and increased flower production in the Cusp Dune suggest favorable conditions for plant growth, likely influenced by frequent sand burial, which enhances plant health and germination potential (Maun, 1998; Bonte et al., 2021; van der Putten and Troelstra, 1990; Huiskes, 1979). This dynamic environment leads to more frequent production of inflorescences compared to the more stable conditions of fixed dunes. Higher canopy height in the North zone of the Cusp Dune suggests landward dune migration, emphasizing its categorization as a more mobile system. In contrast, the Dune Ridge, as part of the fixed dunes, remains more stable (Isermann and Cordes, 1997; Pollmann et al., 2018). The distinction into dynamic and stable systems is also supported by the DEM analysis showing a clear migration for the Cusp Dune and a more stable situation for the Dune Ridge (see also Sect. C1 in the Appendix).

The biomechanical properties of marram grass show some variations between dune types. Young's modulus values indicate higher stiffness on the fixed dune (Dune Ridge), but this trend is not consistently confirmed by stiffness measurements, suggesting that biomechanical differences may not be substantial enough to affect transferability. The absence of clear biomechanical trends across dune types supports the robustness of marram grass in European coastal dune systems, indicating its broad applicability within these environments. However, freshly planted marram grass or newly constructed dunes with planted vegetation may exhibit different biomechanical responses, which should be considered in modeling and practical applications.

4.5 General relevance for foredune vegetation

Marram grass is widely distributed across European sandy coastlines, making our findings highly representative for a broad range of coastal environments. Additionally, closely related species such as *Ammophila breviligulata* in North America share similar ecological functions (Mostow et al., 2021; Stalter and Lonard, 2024). Foredunes, which form the first line of defense against coastal erosion, host a variety of grass species worldwide, many of which exhibit comparable biomechanical adaptations to stabilize sediments and withstand environmental forces (Mostow et al., 2021). Our study provides a valuable framework for understanding the biomechanical differentiation among plant components and their seasonal variations. The observed shifts in stiffness, canopy density, and seasonal growth dynamics are likely key factors for dune stability in other dune grass species as well, underlining the importance of plant trait-based approaches in coastal protection research.

4.6 Methodological considerations

The choice of marram grass for biomechanical parameterization was based on its widespread occurrence, historical use in dune stabilization, and resilience to extreme environmental conditions (Huiskes, 1979; Feagin et al., 2015; de Battisti and Griffin, 2020; Bonte et al., 2021; Strypsteen et al., 2024). Additionally, the species' resilience to high temperatures and drought conditions, as demonstrated by temperature data (see Sect. C4 in the Appendix), makes it an ideal candidate for future coastal defense strategies in the context of climate change (Huiskes, 1979; Gao et al., 2020; Biel and Hacker, 2021). Field investigations revealed seasonal variations in plant morphology, influenced by accretion and erosion processes, but lacked high-resolution Digital Elevation Models (DEMs), highlighting the need for enhanced monitoring methods The interaction between measured canopy height and sand burial dynamics plays a crucial role in understanding vegetation growth, as sediment accumulation can counteract vertical plant developmentLaboratory investigations confirmed that length and outer diameter of plant parts showed minimal seasonal variation, supporting simplified modeling approaches, but also underscored measurement challenges, e.g., due to plant structures with non-circular cross-sections. While stiffness (K_B) emerged as a more reliable parameter than Young's modulus (E), histological analyses emphasized the complexity of plant architecture and the limitations of assuming idealized cross-sectional geometries. Future research should focus on improving the representation of these structural intricacies to enhance biomechanical modeling accuracy.

4.7 Recommendations for future research

To build on the findings of this study and to further enhance our understanding of dune vegetation's biomechanical properties, particularly in the context of coastal protection, several key areas for future research are identified.

- Aboveground vegetation parts, which were the focus of this study's biomechanical parameterization, are crucial for processes such as dune growth and morphological development during the summer. Their sand-trapping properties are essential for dune formation and shaping (Feagin et al., 2015; Ruggiero et al., 2018), and the aboveground biomass creates drag, helping to prevent overwash and, as a result, preventing erosion on the landward side of the dune (Silva et al., 2016). However, belowground plant parts play a critical role in erosion processes and provide lateral resistance of coastal dunes, particularly during extreme events (Feagin et al., 2019; Bryant et al., 2019; de Battisti and Griffin, 2020; Schweiger and Schuettrumpf, 2021; Figlus, 2022). Further data collection on belowground plant parts is needed to enhance our understanding of these processes and the potential impacts of abiotic stress, such as on root development (Gardiner et al., 2016; Kouhen et al., 2023). Implying belowground plant parts in future research was also stressed by Figlus et al. (2014), Silva et al. (2016), and Bryant et al. (2019). Husemann et al. (2024) and Freschet and Roumet (2017) emphasize the importance of considering different parts of the below-ground biomass, such as roots, rhizomes, and buried shoots, each with distinct physical characteristics that contribute to the lateral resistance of coastal dunes, as was done here with aboveground plant parts.

- While this study provides detailed biomechanical insights into marram grass across seasons and dune environments, future research could integrate these findings into aeolian models to assess their practical impact on sediment transport and dune stability. Investigating how variations in plant stiffness, density, and height influence aeolian processes would provide valuable guidance for refining vegetation parameterization in dune modeling frameworks.

- Experiments using real vegetation as well as surrogate models are necessary for comparison and validation, ideally on a large scale. This is particularly important given the challenges in accurately replicating the bending behavior of vegetation. The use of 3D printing or other suitable materials, guided by the biomechanical properties of aboveground plant parts identified in this study, could enhance the accuracy of surrogate models. In this study, it is recommended to model each sprout with four leaves for more accurate representation, although this assumption has not been directly validated within the scope of this research. Therefore, further verification is necessary to confirm this modeling approach and to ensure that it accurately reflects the natural vegetation structure. Additionally, the properties identified in this study must be seasonally distinguished in modeling efforts: summer values should be used for experiments focused on dune accretion processes, while winter values are more appropriate for modeling dune erosion processes. This seasonal differentiation is crucial for accurately simulating the dynamic interactions between vegetation and dune morphology throughout the year.

- Controlled studies on wind exposure effects and comparisons across different sites are recommended to better understand the influence of environmental factors on biomechanical properties. Expanding the dataset to include various locations and environmental conditions will enhance the reliability and applicability of surrogate models. Advanced techniques, such as machine learning, could be incorporated to predict vegetation behavior under diverse conditions. Additionally, a comprehensive comparison with newly constructed dunes planted with marram grass is important. Since marram grass planting is a common practice in coastal protection management (e.g., Gracia et al. (2018)), understanding its biomechanical properties in newly planted scenarios can provide valuable insights for effective dune stabilization strategies.

- While this study employed three-point bending tests due to their practicality and comparability with previous biomechanical studies of vegetation, future research might benefit from exploring two-point bending tests. Two-point bending tests could better simulate natural conditions, such as wind or wave-induced bending of above-ground plant parts. However, these tests are more demanding in terms of sample mounting and alignment, requiring more time and resources than were available in this study. The work of Liu et al. (2021), which employed such tests on salt marsh vegetation, underscores the need for appropriate sample fixation when considering this method.

5 Conclusions

This study provides a comprehensive dataset of the biomechanical properties of marram grass over 12 months, highlighting significant seasonal variations and differences among precisely defined plant components. By analyzing 1543 sprouts, 841 green leaves, 823 brown leaves, and 389 stems, we address the critical need for accurate representations of vegetation in the modeling of dune processes.

- **Seasonal variations and model integration**: The biomechanical properties of marram grass vary seasonally, influencing its role in dune stability. To improve model accuracy, we recommend integrating seasonally adjusted stiffness and density values, as these factors influence sediment capture and dune resilience. Computational models should incorporate temporal shifts in biomechanical traits to reflect changing dune-vegetation interactions.

- **Targeted data collection**: Given the biomechanical differentiation between plant components, field measurements should focus on collecting data on plant structures with the highest seasonal variability, such as flower stems, sprout stiffness, and canopy density. Additionally, repeated seasonal surveys should be prioritized in future monitoring programs. These data will enhance model precision and allow for improved predictions of dune stabilization dynamics.

- **Refinement of wind interaction modeling**: Although our study found no consistent effect of wind on plant biomechanics, future research should further investigate localized wind-vegetation interactions, particularly in environments with high wind variability. While wind exposure is not a key biomechanical driver in our findings, site-specific analyses may be necessary for broader applications.

- **Application to dune management strategie**: The findings reinforce the necessity of adaptive dune management, where seasonal vegetation changes inform conservation and stabilization efforts. Coastal managers should incorporate seasonal shifts in vegetation stiffness and density into dune conservation policies, ensuring that restoration projects align with natural growth cycles to maximize stability.

In conclusion, this study addresses a significant gap in understanding the biomechanical properties of marram grass, providing valuable insights for the development of accurate aboveground vegetation surrogates. The seasonal and plant-part specific traits identified in this research will enhance the reliability of physical and numerical models used to simulate dune dynamics and the role of vegetation in coastal defense. The following table (Table 1) provides a comprehensive overview of these properties, serving as a reference for future modeling efforts aimed at replicating the seasonal variations and structural characteristics essential for accurate dune process simulations.

Table 1. Summary of marram grass parameters for surrogate modeling to accurately represent seasonal variations in dune dynamics and vegetation.

General vegetation traits	**Season**	**Value**		
Canopy height (cm)	Annual	80 ± 15		
Horizontal density (shoots m^{-2})	Summer	494 ± 218		
	Winter	446 ± 210		
Number of flowers (flowers m^{-2})	Summer	109 ± 93		
	Winter	Not applicable		
Plant part		**Length (cm)**	**Outer diameter (mm)**	**Stiffness (N/mm)**
Sprouts	Annual	17 ± 5	3.2 ± 0.5	4.1 ± 1.5
(Green and brown) Leaves	Summer	44 ± 8	1.7 ± 0.2	0.45 ± 0.2
	Winter	50 ± 9		
(Flower) Stems	Summer	65 ± 11	2.8 ± 0.4	5.3 ± 1.7
	Winter	Not applicable		

Data availability. The comprehensive data set presented in this study, detailing individual measurements from the monthly field campaign conducted from January to December 2022 on Spiekeroog, Germany, examining the geometrical and biomechanical properties of marram grass (*Calamagrostis arenaria*, formerly *Ammophila arenaria*), can be found in the following repository: https://doi.org/10.24355/dbbs.084-202404230724-0.

Appendix A: Literature overview

Table A1. Key findings from biomechanical studies combining field observations with three-point bending tests on salt marsh vegetation. Additional methodologies are listed where applicable.

Study	**Key Findings**	**Additional Methodologies**
Rupprecht et al. (2015)	Differences in stiffness observed between various plant species.	-
Rupprecht et al. (2017)	Species-specific stiffness influences wave-vegetation interaction dynamics.	Flume experiments
Vuik et al. (2017)	Integrating a stem breakage model enhances wave attenuation predictions by accounting for seasonal biomass loss and plant breakage.	Numerical modeling
Schulze et al. (2019)	Seasonal differences in stiffness between summer and winter identified across multiple plant species.	-
Zhu et al. (2020)	Seasonal differences (spring, summer, autumn, winter) found to be species- and location-specific.	-
Liu et al. (2021)	Realistic single-stem numerical modeling enabled by a more accurate consideration of the second moment of area.	Histological analysis, Numerical modeling
Paul et al. (2022)	Potential climate change impacts on plant species stiffness and stem diameter highlighted.	-
Keimer et al. (2023)	Seasonal stiffness differences linked to plant morphology; emphasized the need for phenological classification.	-
Keimer et al. (2024)	Seasonal differences observed; initial physical modeling developed based on Cauchy scaling law application.	Surrogate modeling

Appendix B: Plant sampling and methods

B1 Methods overview

Table A2. Overview of literature data on the characteristics of marram grass (*Calamagrostis arenaria*). The reported parameters reflect the terminology used in the respective studies.

Parameter	**Reported Values / Notes**
Height-related parameters	
Growth height (cm)	100 (Bressolier and Thomas, 1977), 80-100 (Hesp, 1981), up to 90 (Mostow et al., 2021)
Tiller height (cm)	up to 75 (Hacker et al., 2012)
Stem height (mm)	up to 195 (Feagin et al., 2019)
Panicle length (cm)	up to 200 (Mostow et al., 2021)
Density-related parameters	
Horizontal density (tillers/m^2)	556 (Biel et al., 2019), up to 1000 (Zarnetske et al., 2012)
Stem density (stems/m^2)	260 (Feagin et al., 2019), 203 (Seabloom and Wiedemann, 1994)
Plant number per m^2	480 (Hacker et al., 2012)
Tiller density (tillers per rhizome)	up to 3 (Hacker et al., 2012)
Leaves per m^2	1516 ± 8 (Feagin et al., 2019)
Morphological traits	
Shoots per plant	up to 4 (Mostow et al., 2021)
Leaves per stem	1 ± 3 (Feagin et al., 2019)
Stem diameter (mm)	3 ± 1 (Feagin et al., 2019)
Leaf area (mm^2)	1605 ± 7 (Feagin et al., 2019)
Leaf width (cm)	up to 5 (Mostow et al., 2021)
Aboveground biomass	
Tiller weight (g)	up to 4 (Hacker et al., 2012)
Belowground biomass	
Belowground biomass (g)	up to 100 (de Battisti and Griffin, 2020)
Fine roots (g/m^2)	288 ± 14 (Feagin et al., 2019)
Histological examinations	
Histological studies	Analysis of cell structures (Andrade et al., 2021); tissue properties (Chergui et al., 2017)

A1 Plant sampling

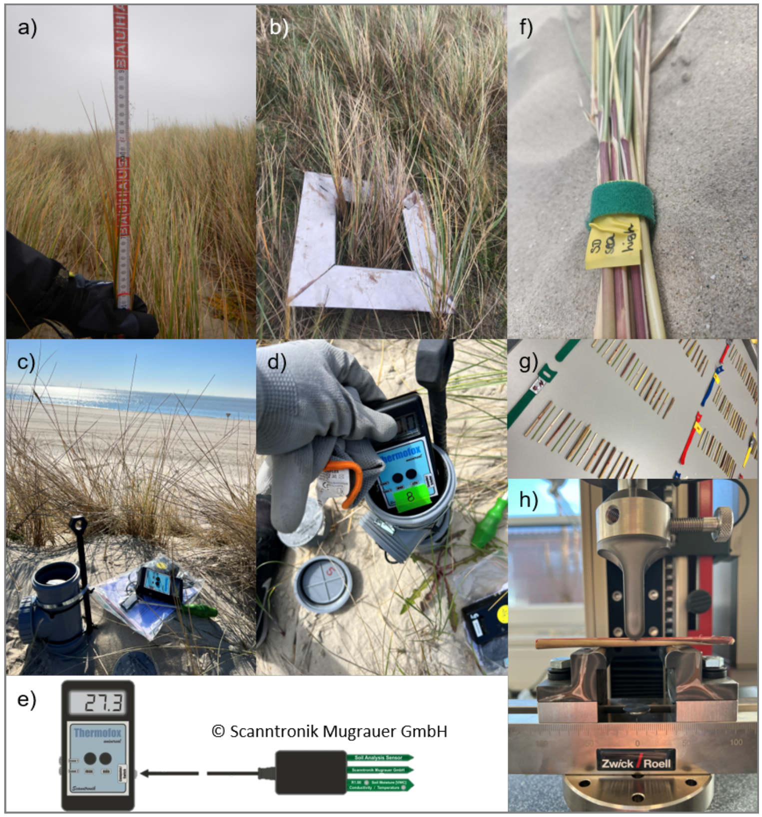

Figure A1. Overview of the methodology used in this study. (a) Measurement of canopy height using a folding ruler. (b) Determination of horizontal density with a 20 cm frame. (c) Replacement of the data logger connected to the soil analysis sensor, with a close-up view in (d) showing the data logger within its enclosure during replacement. (e) Manufacturer's overview (Scanntronik Mugrauer GmbH, 2024a) of the data logger (left) connected to the soil analysis sensor (right), which is installed approximately $20 - 30$ cm deep in the soil. (f) Bundle of plant samples collected for further laboratory analysis. (g) Sample sections prepared for three-point bending tests. (h) Image of a sample in place for a three-point bending test before the start of the experiment.

B1 Plant measurements

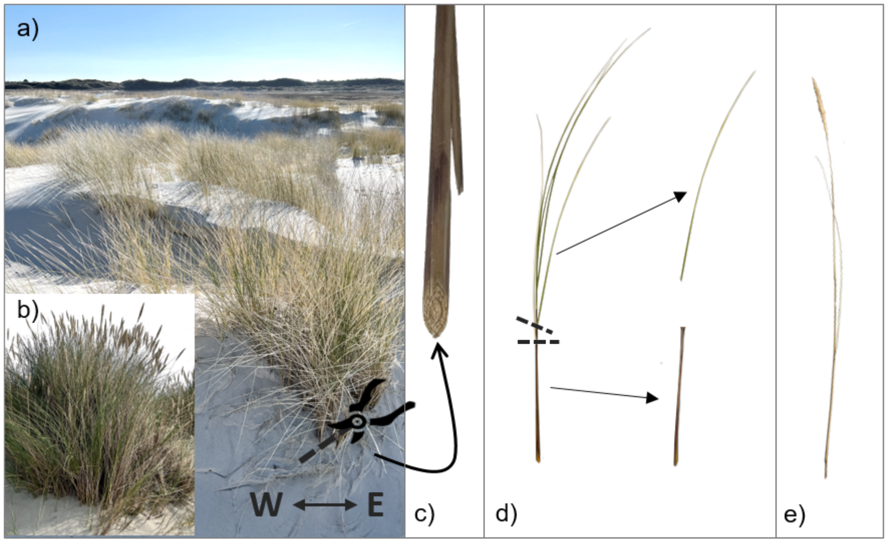

Figure B1. Overview of sample collection and preparation of marram grass. (a) Typical view of marram grass in winter (March 2022) with an illustration of the angled cutting technique used to ensure that the orientation of the samples in the field is maintained in the laboratory. Samples were cut and collected at the height of the soil surface. (b) Marram grass in summer (August 2022) showing high density and the presence of flowering stems. (c) Close-up of the cut end of a sample, indicating the longer side facing west. (d) A full shoot sample with cut sections for the removal of green/brown leaves (top) and sprouts (bottom), which are present year-round. (e) Separate image of a flowering stem after removal, relevant for the summer state of marram grass.

Appendix C: Environmental parameters

Morphologic changes for the two field sites have been assessed based on DEM model data for the areas sourced from the NLWKN (2024) for the years 2019 and 2022. Deriving a difference map for the two DEMs yields vertical elevation changes between those two surveys for the two field sites, Dune Ridge and Cusp Dune. Furthermore, environmental parameters included weather data that were used to further describe the environmental conditions at study sites. The weather data included wind measurements at $10\,\text{m}$ height, air temperature, and precipitation for the years 2017-2022, with a particular focus on wind data due to its presumed relevance to the biomechanical properties of the vegetation and its influence on accretion processes. Wind data were obtained from a weather station operated by the Deutscher Wetterdienst (DWD), located at $53.7674°N, 7.6721°E$ on Spiekeroog. Air temperature and precipitation data were sourced from another weather station operated by the Institute for Chemistry and Biology of the Marine Environment (ICBM) of the University of Oldenburg, located nearby at $53.7762°N, 7.6880°E$. Notably, all measurements were recorded at 10-minute intervals. Temperature and precipitation data was subsequently averaged to monthly mean values. In addition to the weather data, soil temperature measurements were taken at a depth of $20-30\,\text{cm}$ using Soil Analysis Sensors (Digital) by Scanntronik Mugrauer GmbH. The measurement range for the temperature was -30 řC to $+80$ řC, with an average resolution of 0.1 řC and an accuracy of $+/-1$ řC. The posi-

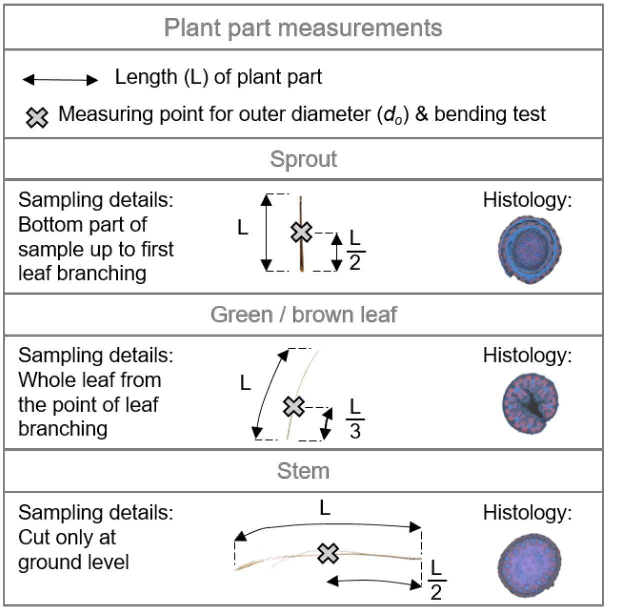

Figure B2. Illustration of length (L) measurements, indicated by arrows, and measuring points marked with an "X" for defining the outer diameter (d_o) and the location of three-point bending tests. These measurements are demonstrated for the three plant component types: sprout, green/brown leaf, and (flowering) stem. Additionally, histological cross-sections are provided for each plant part to highlight the complexity of their internal structures.

tions of these sensors are marked in Figures 2a and 3a. Soil temperature was recorded at 10-minute intervals with a Thermofox Universal data logger by Scanntronik Mugrauer GmbH, using Softfox (version 3.05) for setup. These recordings were first averaged over 60-minute periods to calculate hourly temperatures. For analysis purposes, the hourly temperatures were subsequently categorized into daytime and nighttime temperatures. Daytime temperatures were defined as those recorded between 06:00 and 17:59, while nighttime temperatures were defined as those recorded between 18:00 and 05:59. This separation of data allowed for a detailed examination of diurnal temperature variations and their potential impact on dune vegetation. Due to a sensor failure at the Cusp Dune, there was a significant data loss from May 2nd to July 13th, likely affecting the recorded temperatures in May, June, and July.

C1 Morphology

For the Cusp Dune situated at the northern beach of the island a clear southward migration can be identified based on the compiled sedimentation erosion maps shown in Fig. C1a. The northern part of the dune along the luv or seaward side being the most exposed part, is eroded up to -2.9 m within three years becoming level with the beach north of it. The former dune toe zone has migrated 28 m inland between 2019 and 2022. The central and southern part of the Cusp Dune shows significant vertical accretion with an average of +1.5 m over three years. Apart from the dune itself, the beach north of it shows erosion of an average -0.4 m during this period. Meanwhile, the blow outs left and right of the Cusp Dune show accretion of 0.5 m along the western blowout and 0.6 m on average along the eastern blowout. This overall pattern clearly mimics the impact of the predominant north-western angle of wave and wind attack, eroding the northern beach and exposed dune slopes, while accumulating sediments within the more sheltered blow out sections and on the lee ward side of the dune ridges.

In addition to the sedimentation-erosion maps, aeolian transport volume for the field site has been calculated and is compiled in Fig. C1b with monthly intervals. The calculation is based on the revised transport formulae found in (van Rijn and Strypsteen, 2020). Wind speed and direction have been sourced from the weather station 6091 No. operated by the German Weather Service (DWD), located at $53.7674°N, 7.6721°E$ on Spiekeroog. Transport volumes are calculated with the formulae and consider wind angle of attack in relation to the dune location, exposure and area. For the Cusp Dune a total of 1606 m^3 was calculated, which equates to 0.3 m elevation increase per year on average, well corresponding to the DEM values.

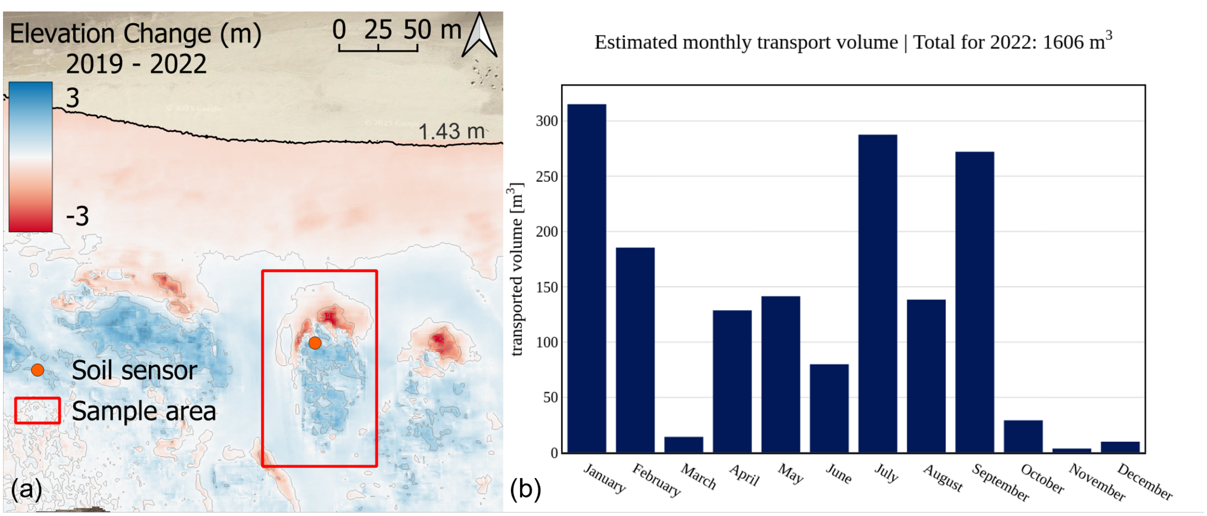

Figure C1. Morphological changes 2019 - 2022 for the cusp dune (a) based on DEM data with a 1 mx1 m raster resolution provided by the Lower Saxony Water Management, Coastal and Nature Protection Agency (NLWKN). Aeolian transport volume calculation for 2022 based on wind speed and direction data sourced from the German Weather Service (DWD) station on Spiekeroog situated between the two field sites.

In comparison, the southern Dune Ridge is relatively stable over multiple years, which is expressed in a gradual vertical increase of 0.3-0.7 m along the ridge line and larger depositions on the lee side with up to 1.4 m (see Figure C2a). Maximum erosion occurs near the luv side dune toe area ranging between -0.4 m and -1.2 m. The beach in front of the dune shows gradual vertical increase with an average 0.2 m m over three years.

The aeolian transport volume calculated the same way for the dune ridge yields a total sedimentation volume of 2225 m^3 per year, which corresponds to a vertical increase of 0.6 m. This value is higher than for the cusp dune site but still within the DEM range for the period. From the map in Figure C2a the blow out is clearly visible in the middle of the dune ridge sampling area, which exhibits strong erosion, while the surrounding crest and land ward side of the dune experience sedimentation, corroborating the average net sedimentation value.

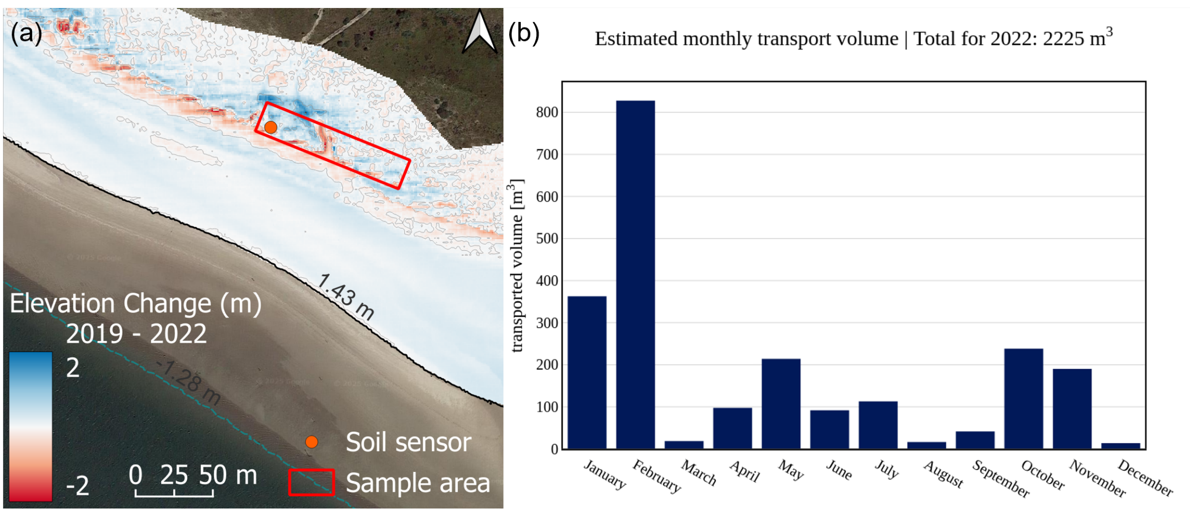

Figure C2. Morphological changes 2019 - 2022 for Dune Ridge (a) based on DEM data with a 1 mx1 m raster resolution provided by the Lower Saxony Water Management, Coastal and Nature Protection Agency (NLWKN). Aeolian transport volume calculation for 2022 based on wind speed and direction data sourced from the German Weather Service (DWD) station on Spiekeroog situated between the two field sites.

Both field sites were exposed to five storm surge events during 2022 of which all five reached the dune toe areas and induced erosion (BSH, 2024).

C2 Wind forces

The wind roses (Fig. C3) illustrate the distribution of wind speed and direction for the years 2018-2022 (Fig. C3a) and the year 2022 (Fig. C3b), along with seasonal data for 2022 (i.e., summer and winter, see Figure C3c and d). During the years 2018-2022, strong winds (> 8 m/s, *Bft* 5) were west-dominated, totaling 64.46 % (W: 24.43 %, NW: 22.71 %, SW: 17.32 %).

In 2022, the distribution of strong winds shifted slightly, but remained west-dominated, totaling 66.61 % (W: 24.27 %, NW: 26.59 %, SW: 15.75 %).

Focusing on summer months (April to September 2022), which represent key growth phases for vegetation, strong winds were predominantly from the northwest (W: 25.85 %, NW: 38.62 %). Moderate winds (< 8 m/s) were more evenly distributed, ranging from 8.52 % (SW) to 17.11 % (E).

In winter (October to March 2022), strong winds were more distributed and shifted slightly to the southwest (W: 22.97 %, SW: 22.00 %, NW: 16.70 %). Moderate winds were predominantly from the south (S: 29.39 %, SE: 19.39 %, SW: 14.61 %).

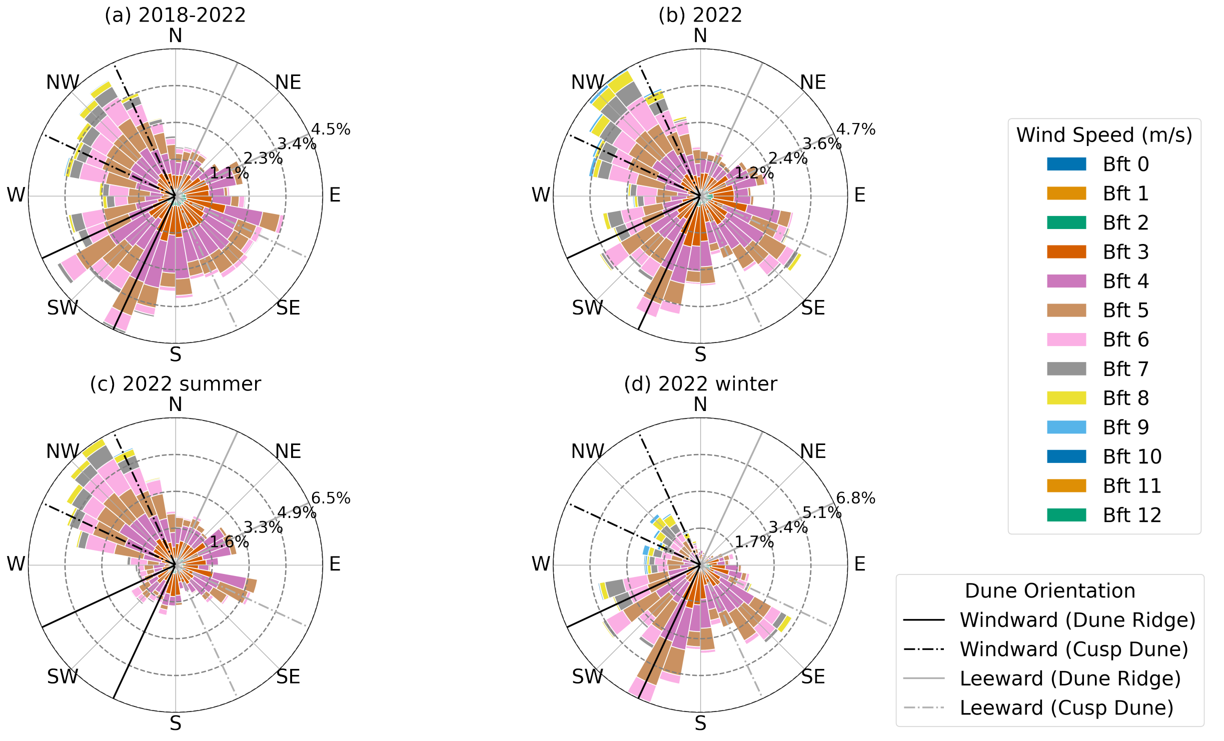

Figure C3. Wind roses showing wind direction and frequency for various time periods (Deutscher Wetterdienst): (a) wind rose for 2018-2022, (b) wind rose for 2022, (c) wind rose for summer months of 2022 (April-September), (d) wind rose for winter months of 2022 (October-March). Windward (black) and leeward (light gray) directions are indicated for each dune site. Solid lines represent Dune Ridge, and dot-dashed lines represent Cusp Dune, highlighting the directions perpendicular to the wind-exposed and wind-sheltered dune sides.

C3 Climate

The analysis of air temperature and precipitation data revealed that the air temperature peaks were consistently reached in July or August across all years, with August being the peak month in 2022 (Fig. C4). The lowest temperatures were observed from November to March in all years, with the winter of 2022 being relatively mild compared to other years, except for December. Overall, the air temperatures in 2022 were within the average range. Regarding precipitation, the data showed that 2022 had generally average precipitation levels with some outliers. Notably, February 2022 had a marked peak, recording the highest monthly average precipitation among all observed years.

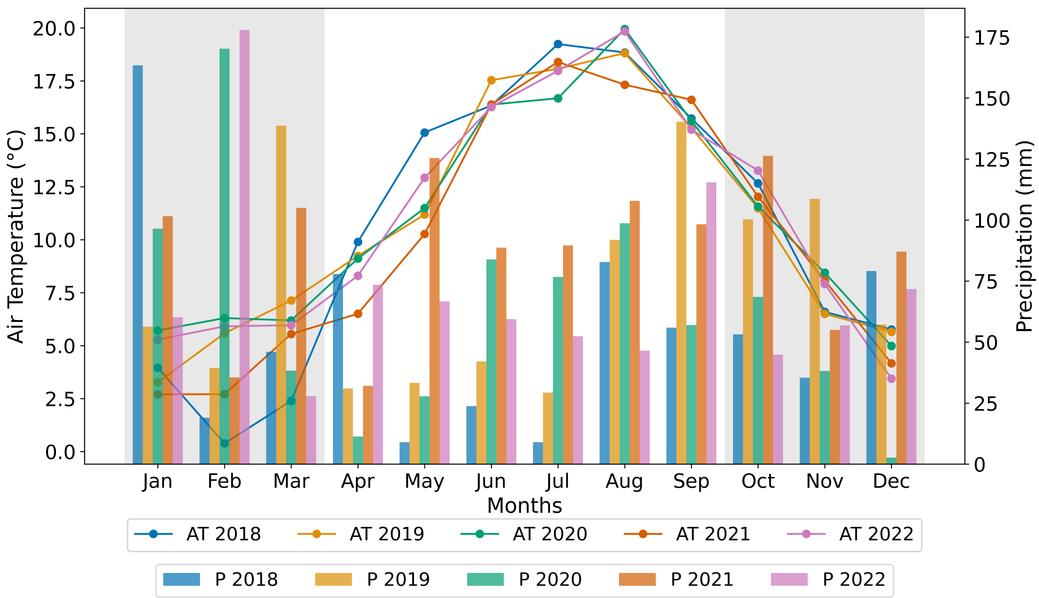

Figure C4. Markers and lines are showing monthly mean values of air temperature (in C) and the bars monthly values of precipitation (in mm) for the years 2018-2022. White and gray background color indicate the definition of summer and winter months, respectively.

C4 Soil sensor

The soil temperatures at Dune Ridge and Cusp Dune sites showed considerable seasonal and diurnal variations throughout the year 2022, as illustrated by the boxplots in Fig. C5.

Comparing the two sites, Dune Ridge (Fig. C5a) generally exhibited higher temperature extremes, especially during the day, reflecting potentially greater solar exposure due to sparse vegetation. For instance, in August, the maximum daytime soil temperature at Dune Ridge was 48.03 řC with an average of 28.02 řC, while at Cusp Dune (Fig. C3b), the maximum was 31.60 řC with an average of 23.30 řC. The highest daytime soil temperature recorded was 53.38 řC at Dune Ridge in July. The surrounding vegetation at Cusp Dune, which grew tall and dense by June (Fig. C4-2a and -2b), likely shaded the sensor, contributing to lower recorded temperatures compared to Dune Ridge (Fig. C6-1a and -b).

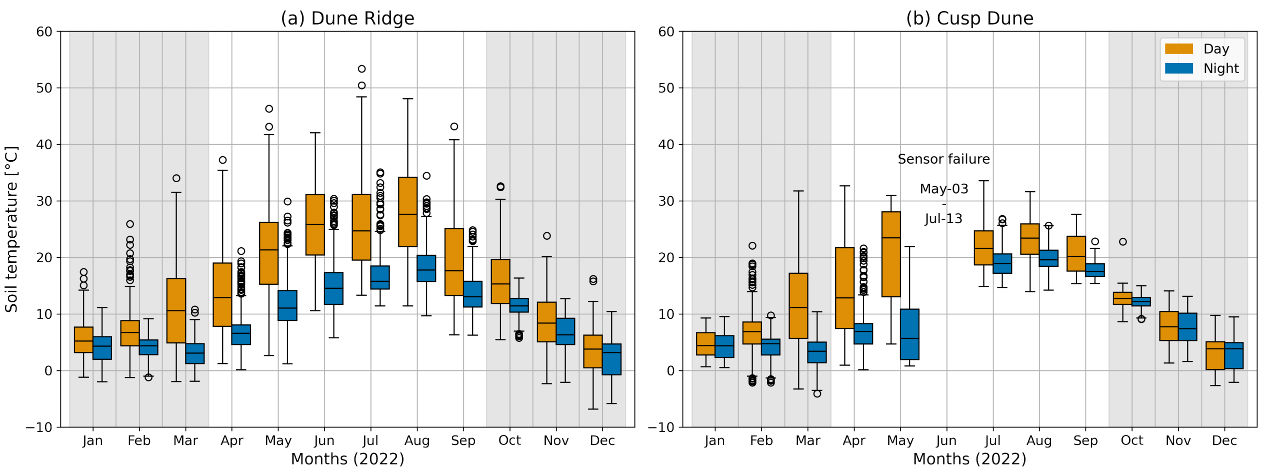

Figure C5. Monthly daytime (in orange) and nighttime soil temperatures (in blue) at (a) Dune Ridge and (b) Cusp Dune throughout 2022. White and gray background color indicate the definition of summer and winter months, respectively.

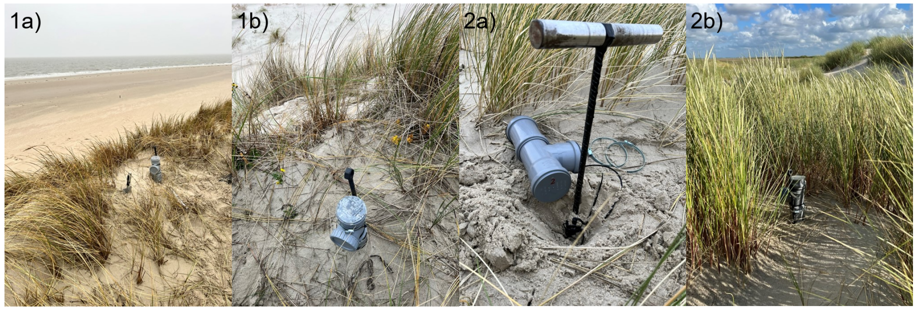

Figure C6. (1) Soil sensor at Dune Ridge (1a) in February 2022 and (1b) in November 2022. (2) Soil sensor at Cusp Dune (2a) in February 2022 and (2b) in June 2022. The images illustrate the differences in vegetation cover and shading at the sensor locations across different times of the year.

Appendix D: Biomechanical properties

This section provides a comprehensive overview of the seasonal variations in the biomechanical properties of aboveground vegetation parts of marram grass. The analysis begins with summary tables (see Tables D1-D6) presenting the results of the statistical analyses, structured to address the key research questions and highlight significant differences in biomechanical traits. Following this, supplementary figures (see Figures C5-D1) offer a visual representation of these findings through heatmaps, illustrating the spatial and seasonal variations of the measured properties across different dune zones.

D1 Seasonal variations in biomechanical properties of marram grass

Table D1. Mean and standard deviation of canopy height, horizontal density, and number of flowers for both dune sites across seasons (summer/winter) as well as Mann-Whitney U test results showing seasonal differences with significant values (p<0.05) in bold.

Parameter	**Unit**	**Season**	**mean**	**std**	**P-value**	n
Canopy Height	[cm]	summer	79.66	15.62	0.343	707
		winter	79.87	13.38		705
Horizontal Density	[shoots m^{-2}]	summer	493.49	217.97	**<0.001**	707
		winter	445.65	209.93		603
Number of Flowers	[flowers m^{-2}]	summer	108.86	92.50	**NaN**	306
		winter	NaN	NaN		

Table D2. Mean and standard deviation of parameters for different plant components and dune sites across seasons (summer/winter).

			Stiffness K_B		Young's modulus E		Outer diameter d_o		Length L	
			[N/mm]		**[MPa]**		**[mm]**		**[cm]**	
Plant part	**Dune site**	**Season**	**mean**	**std**	**mean**	**std**	**mean**	**std**	**mean**	**std**
Sprout	Combined	summer	3.98	1.46	1175.85	563.72	3.24	0.53	18.28	5.11
	Combined	winter	4.15	1.59	1173.47	479.92	3.10	0.51	15.37	4.45
	Dune Ridge	summer	3.83	1.46	1252.04	649.42	3.14	0.51	19.04	5.11
	Dune Ridge	winter	4.19	1.53	1209.69	453.96	3.15	0.48	14.86	3.92
	Cusp Dune	summer	4.06	1.46	1134.94	518.45	3.29	0.54	17.90	5.12
	Cusp Dune	winter	4.14	1.62	1155.97	492.47	3.07	0.52	15.62	4.70
Green Leaf	Combined	summer	0.29	0.11	1215.16	526.92	1.69	0.22	44.35	8.14
	Combined	winter	0.33	0.13	1585.21	624.35	1.57	0.20	51.47	8.94
	Dune Ridge	summer	0.29	0.11	1379.62	609.47	1.63	0.23	43.14	9.02
	Dune Ridge	winter	0.32	0.13	1755.47	626.07	1.52	0.21	50.84	8.12
	Cusp Dune	summer	0.29	0.11	1132.93	485.64	1.72	0.22	44.95	7.70
	Cusp Dune	winter	0.33	0.12	1502.92	623.52	1.59	0.20	51.77	9.33
Brown Leaf	Combined	summer	0.70	0.46	1790.77	809.09	1.72	0.26	43.80	6.93
	Combined	winter	0.47	0.18	1837.46	855.73	1.67	0.21	47.82	7.95
	Dune Ridge	summer	0.81	0.55	2248.17	1100.85	1.69	0.28	43.80	8.04
	Dune Ridge	winter	0.48	0.18	2159.45	943.93	1.61	0.24	46.43	8.62
	Cusp Dune	summer	0.64	0.41	1550.03	655.26	1.73	0.24	43.80	6.38
	Cusp Dune	winter	0.46	0.18	1681.84	813.11	1.70	0.20	48.47	7.64
Stem	Combined	summer	5.30	1.65	2641.05	1152.78	2.78	0.39	64.94	10.87
	Dune Ridge	summer	5.13	1.48	2776.14	1002.39	2.69	0.32	65.42	9.47
	Cusp Dune	summer	5.39	1.74	2573.51	1230.58	2.83	0.43	64.70	11.57

D2 Comparison of biomechanical traits among plant parts

D3 Impact of wind exposure on biomechanical traits

D4 Influence of dune systems on plant biomechanics

Table D3. Mann-Whitney U Test results comparing seasonal differences (summer/winter) for each plant component, with data aggregated across both dune sites (Dune Ridge and Cusp Dune). Significant values (p<0.05) in bold.

Part	Parameter	P-Value	n_{summer}	n_{winter}
Sprout	Stiffness K_B	**<0.001**	641	792
	Young's modulus E	**<0.001**	641	792
	Outer diameter d_o	0.909	641	792
	Length L	0.196	619	705
Green Leaf	Stiffness K_B	**<0.001**	269	460
	Young's modulus E	**<0.001**	269	460
	Outer diameter d_o	**<0.001**	269	460
	Length L	**<0.001**	270	477
Brown Leaf	Stiffness K_B	0.077	250	462
	Young's modulus E	0.898	250	462
	Outer diameter d_o	0.199	250	462
	Length L	**<0.001**	253	458

D5 Supplementary figures

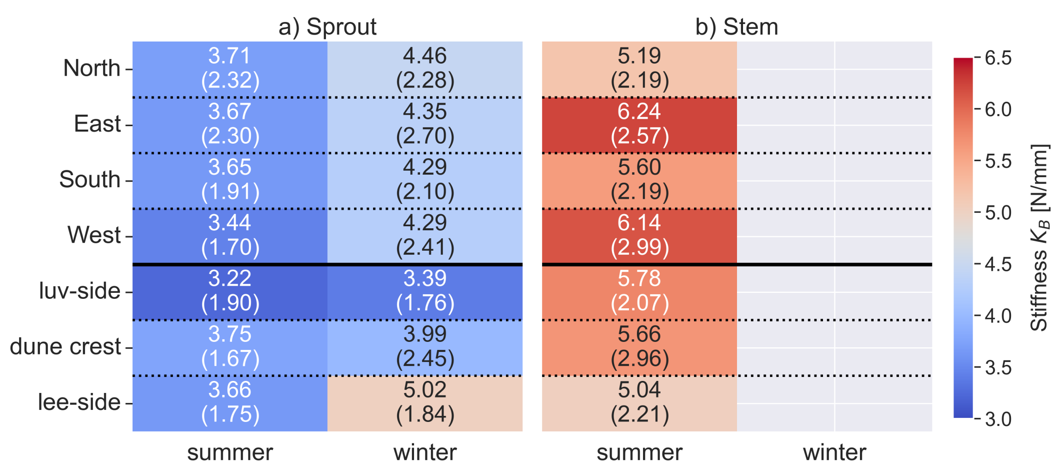

Figure D1. Heatmap showing stiffness K_B for (a) sprout and (b) stem in different zones and seasons. The values within the heatmap cells represent the mean stiffness (in $\mathrm{N/mm}$) with the standard deviation in parentheses.

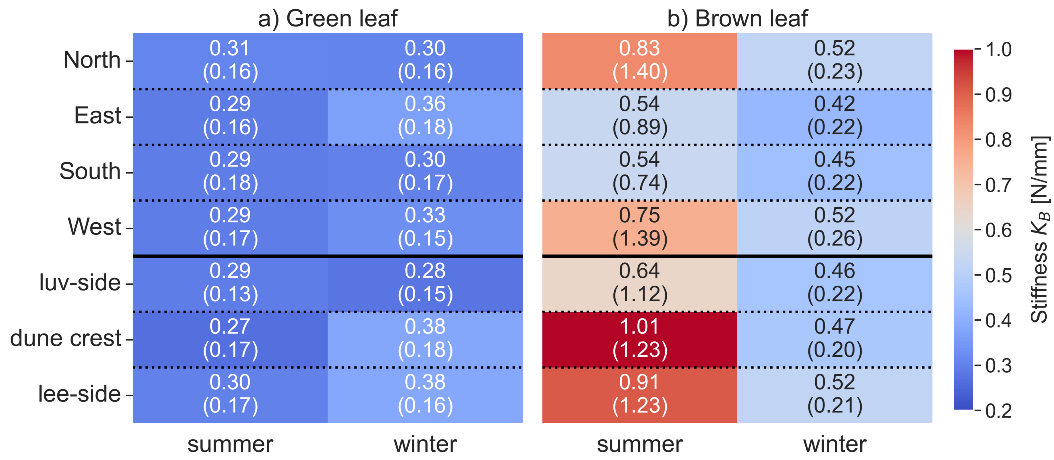

Figure D2. Heatmap showing stiffness K_B for (a) green leaf and (b) brown leaf in different zones and seasons. The values within the heatmap cells represent the mean stiffness (in $\mathrm{N/mm}$) with the standard deviation in parentheses.

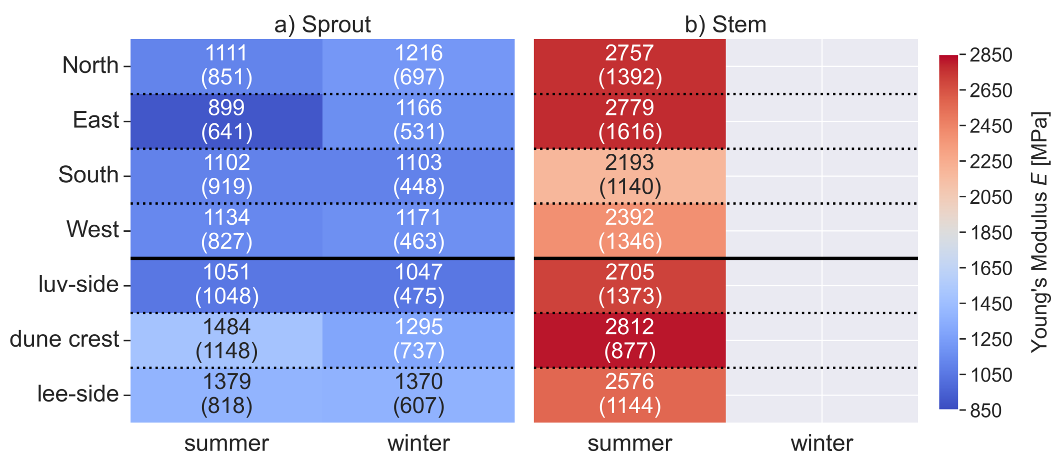

Figure D3. Heatmap showing Young's modulus E for (a) sprout and (b) stem in different zones and seasons. The values within the heatmap cells represent the mean Young's modulus (in MPa) with the standard deviation in parentheses.

Table D4. Results of the Mann-Whitney U tests comparing biomechanical parameters between plant components for each season. Significant values (p<0.05) in bold.

Part A	Part B	Season	Parameter	P-Value	n_A	n_B	Part A	Part B	Season	Parameter	P-Value	n_A	n_B
Sprout	Stem	summer	K_B	**<0.001**	641	253	Green Leaf	Brown Leaf	summer	K_B	**<0.001**	269	250
			E	**<0.001**	641	253				E	**<0.001**	269	250
			d_o	**<0.001**	641	253				d_o	0.830	269	250
			L	**<0.001**	619	254				L	0.611	270	253
Sprout	Green Leaf	summer	K_B	**<0.001**	641	269	Green Leaf	Brown Leaf	winter	K_B	**<0.001**	460	462
			E	0.319	641	269				E	0.399	460	462
			d_o	**<0.001**	641	269				d_o	**<0.001**	460	462
			L	**<0.001**	619	270				L	**<0.001**	477	458
Sprout	Green Leaf	winter	K_B	**<0.001**	792	460	Green Leaf	Stem	summer	K_B	**<0.001**	269	253
			E	**<0.001**	792	460				E	**<0.001**	269	253
			d_o	**<0.001**	792	460				d_o	**<0.001**	269	253
			L	**<0.001**	705	477				L	**<0.001**	270	254
Sprout	Brown Leaf	summer	K_B	**<0.001**	641	250	Brown Leaf	Stem	summer	K_B	**<0.001**	250	253
			E	**<0.001**	641	250				E	**<0.001**	250	253
			d_o	**<0.001**	641	250				d_o	**<0.001**	250	253
			L	**<0.001**	619	253				L	**<0.001**	253	254
Sprout	Brown Leaf	winter	K_B	**<0.001**	792	462							
			E	**<0.001**	792	462							
			d_o	**<0.001**	792	462							
			L	**<0.001**	705	458							

Table D5. Mann-Whitney U Test results comparing plant components between different exposure conditions at each dune site. For Dune Ridge, comparisons are made between luv and lee, while for Cusp Dune, comparisons are made between Northwest and Southeast. Significant values (p<0.05) in bold.

Dune site	**Zone 1**	**Zone 2**	**Part**	**Parameter**	**P-Value**	$\mathbf{n_{Zone1}}$	$\mathbf{n_{Zone2}}$
Dune Ridge	luv	lee	Sprout	Stiffness K_B	**<0.001**	199	190
				Young's modulus E	**<0.001**	199	190
				Outer diameter d_o	0.957	199	190
				Length L	0.168	177	173
			Green Leaf	Stiffness K_B	**0.010**	91	90
				Young's modulus E	**0.002**	91	90
				Outer diameter d_o	0.622	91	90
				Length L	**<0.001**	101	90
			Brown Leaf	Stiffness K_B	0.125	89	88
				Young's modulus E	0.689	89	88
				Outer diameter d_o	0.183	89	88
				Length L	**0.003**	78	88
			Stem	Stiffness K_B	0.086	31	38
				Young's modulus E	0.642	31	38
				Outer diameter d_o	0.668	31	38
				Length L	0.159	31	39
Cusp Dune	Northwest	Southeast	Sprout	Stiffness K_B	0.748	472	482
				Young's modulus E	**0.020**	472	482
				Outer diameter d_o	0.316	472	482
				Length L	**0.015**	444	452
			Green Leaf	Stiffness K_B	0.506	261	253
				Young's modulus E	0.055	261	253
				Outer diameter d_o	**0.030**	261	253
				Length L	0.165	263	258
			Brown Leaf	Stiffness K_B	**0.002**	253	247
				Young's modulus E	**0.015**	253	247
				Outer diameter d_o	0.960	253	247
				Length L	0.568	259	251
			Stem	Stiffness K_B	0.597	124	113
				Young's modulus E	0.744	124	113
				Outer diameter d_o	0.526	124	113
				Length L	0.260	123	111

Table D6. Mann-Whitney U Test results comparing Dune Ridge (Zone 1) with Cusp Dune (Zone 2) for each plant component. Significant values (p<0.05) in bold.

Part	Parameter	P-Value	n_{Zone1}	n_{Zone2}
Sprout	Stiffness K_B	0.347	479	954
	Young's modulus E	**0.002**	479	954
	Outer diameter d_o	**0.044**	479	954
	Length L	**0.039**	428	896
Green Leaf	Stiffness K_B	0.872	215	514
	Young's modulus E	**0.031**	215	514
	Outer diameter d_o	0.063	215	514
	Length L	0.277	226	521
Brown Leaf	Stiffness K_B	**0.036**	212	500
	Young's modulus E	**<0.001**	212	500
	Outer diameter d_o	**<0.001**	212	500
	Length L	**0.010**	201	510
Stem	Stiffness K_B	0.439	84	237
	Young's modulus E	0.185	84	237
	Outer diameter d_o	0.061	84	237
	Length L	0.805	85	234

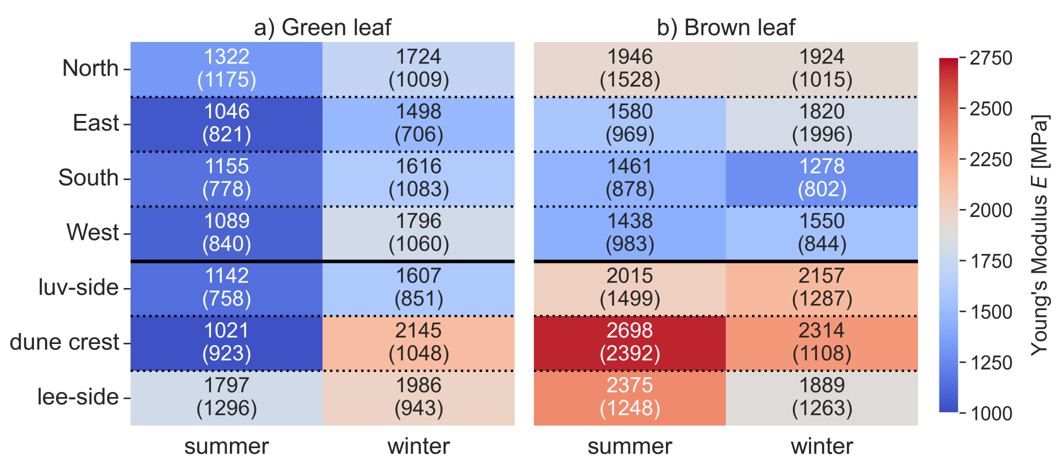

Figure D4. Heatmap showing Young's modulus E for (a) green leaf and (b) brown leaf in different zones and seasons. The values within the heatmap cells represent the mean Young's modulus (in MPa) with the standard deviation in parentheses.

Author contributions. VK, OL, and KK planned the campaign; VK, OL, and LA performed the measurements; VK, JC, and BS analyzed the data; VK wrote the manuscript draft; VK and OL prepared visualizations; OL, JC, KK, LA, BM, DS, BS, and NG reviewed and edited the manuscript; OL, DS, and NG administered the project and organized funding acquisition.

Competing interests. The authors declare that they have no conflict of interest.

Acknowledgements. This study was performed as part of the joint research project Gute Küste Niedersachsen funded by the Lower-Saxony Ministry of Research and Culture (FKZ: 76251-17-5/19) and the Volkswagen Stiftung. We are greatly indebted to the National Park Authority (Nationalparkverwaltung Niedersächsisches Wattenmeer) for providing site access and permission to use it for scientific research. We would also like to thank Mr. Malte Kumlehn and Mr. Leon Vinkelau, for assisting with field campaigns as well as supporting in the laboratory. The authors wish to thank Dipl. Phys. Frank Hillmann from the ICBM, University of Oldenburg, for providing weather data from Spiekeroog. Appreciation is also extended to Prof. Robert Hänsch from the Institute of Plant Biology at TU Braunschweig for valuable discussions about plant morphology. Special thanks go to Holger Dirks from the Coastal Research station of the Niedersächsischer Landesbetrieb für Wasserwirtschaft, Küsten- und Naturschutz (NLWKN) for providing high resolution digital elevation model data of Spiekeroog.

References

Andrade, T., Beirão, J., Arruda, A., and Cruz, C.: The adaptive power of Ammophila arenaria: biomimetic study, systematic observation, parametric design and experimental tests with bimetal, Polymers, 13, https://doi.org/10.3390/polym13152554, 2021.

Baas, A. and Nield, J. M.: Ecogeomorphic state variables and phasespace construction for quantifying the evolution of vegetated aeolian landscapes, Earth Surface Processes and Landforms, 35, 717–731, https://doi.org/10.1002/esp.1990, 2010.

Bakker, J.: Ecology of salt marshes: 40 years of research in the Wadden Sea, Wadden Academy, Leeuwarden, ISBN 9789490289324, 2014.

Barbier, E. B., Hacker, S. D., Kennedy, C., Koch, E. W., Stier, A. C., and Silliman, B. R.: The value of estuarine and coastal ecosystem services, Ecological monographs, 81, 169–193, 2011.

Bauer, D. F.: Constructing confidence sets using rank statistics, Journal of the American Statistical Association, 67, 687–690, https://doi.org/10.1080/01621459.1972.10481279, 1972.

Biel, R. G. and Hacker, S. D.: Climate Change Alters The Interaction of Two Invasive Beachgrasses With Implications For Range Shifts And Coastal Dune Functions, https://doi.org/10.21203/rs.3.rs-529207/v1, 2021.

Biel, R. G., Hacker, S. D., and Ruggiero, P.: Elucidating Coastal Foredune Ecomorphodynamics in the U.S. Pacific Northwest via Bayesian Networks, Journal of Geophysical Research: Earth Surface, 124, 1919–1938, https://doi.org/10.1029/2018JF004758, 2019.

Bonte, D., Batsleer, F., Provoost, S., Reijers, V., Vandegehuchte, M. L., van de Walle, R., Dan, S., Matheve, H., Rauwoens, P., Strypsteen, G., Suzuki, T., Verwaest, T., and Hillaert, J.: Biomorphogenic feedbacks and the spatial organisation of a dominant grass steer dune development, Frontiers in Ecology and Evolution, 11, https://doi.org/10.3389/fevo.2021.761336, 2021.

Boorman, L. A.: The grazing management of sand dunes: Handbook: (Unpublished), 1988.

Bouma, T. J., de Vries, M. B., Low, E., Peralta, G., Tánczos, I. C., van de Koppel, J., and Herman, P. M. J.: Trade-Offs related to ecosystem engineering: A case study on stiffness of emerging macrophytes, Ecology, 86, 2187–2199, https://doi.org/10.1890/04-1588, 2005.

Bouma, T. J., Temmerman, S., van Duren, L. A., Martini, E., Vandenbruwaene, W., Callaghan, D. P., Balke, T., Biermans, G., Klaassen, P. C., van Steeg, P., Dekker, F., van de Koppel, J., de Vries, M. B., and Herman, P.: Organism traits determine the strength of scale-dependent bio-geomorphic feedbacks: A flume study on three intertidal plant species, Geomorphology, 180-181, 57–65, https://doi.org/10.1016/j.geomorph.2012.09.005, 2013.

Bouma, T. J., van Belzen, J., Balke, T., Zhu, Z., Airoldi, L. Blight, A. J., Davies, A. J., Galvan, C., Hawkins, S. J., Hoggart, S. P. G., Lara, J. L., Losada, I. J., Maza, M., Ondiviela, B., Skov, M. W., Strain. E. M., Thompson, R. C., and Yang, S. Herman, P. M. J.: Identifying knowledge gaps hampering application of intertidal habitats in coastal protection: Opportunities & steps to take, Coastal Engineering, 87, 147–157, https://doi.org/10.1016/j.coastaleng.2013.11.014, 2014.

Bressolier, C. and Thomas, Y.-F.: Studies on Wind and Plant Interactions on French Atlantic Coastal Dunes, Journal of Sedimentary Petrology, 47, 331–338, 1977.

Bryant, D. B., Anderson Bryant, M., Sharp, J. A., Bell, G. L., and Moore, C.: The response of vegetated dunes to wave attack, Coastal Engineering, 152, 103 506, https://doi.org/10.1016/j.coastaleng.2019.103506, 2019.

BSH: Sturmfluten: Berichte zu Sturmfluten und extremen Wasserständen, https://www.bsh.de/DE/THEMEN/Wasserstand_und_Gezeiten/Sturmfluten/sturmfluten_node.htm, 2024.

Carter, R. W. G.: Near-future sea level impacts on coastal dune landscapes, Landscape Ecology, 6, 29–39, https://doi.org/10.1007/BF00157742, 1991.

Chergui, A., El Hafid, L., and Melhaoui, M.: Characteristics of marram grass (Ammophila arenaria L.), plant of the coastal dunes of the Mediterranean Eastern Morocco: Ecological, morpho-anatomical and physiological aspects, Journal of Materials and Environmental Sciences, 8, 3759–3765, 2017.

Davidson, S. G., Hesp, P. A., and Da Silva, G. M.: Controls on dune scarping, Progress in Physical Geography, 44, 923–947, https://doi.org/10.1177/0309133320932880, 2020.

Davis, J. H.: Dune formation and stabilization by vegetation and plantings, Coastal Engineering Proceedings, 1, 29, https://doi.org/10.9753/icce.v6.29, 2011.

de Battisti, D.: The resilience of coastal ecosystems: A functional trait–based perspective, Journal of Ecology, 109, 3133–3146, https://doi.org/10.1111/1365-2745.13641, 2021.

de Battisti, D. and Griffin, J. N.: Below-ground biomass of plants, with a key contribution of buried shoots, increases foredune resistance to wave swash, Annals of Botany, 125, 325–334, https://doi.org/10.1093/aob/mcz125, 2020.

de Jong, B., Keijsers, J. G. S., Riksen, M. J. P. M., Krol, J., and Slim, P. A.: Soft engineering vs a dynamic approach in coastal dune management: A case study on the North Sea Barrier Island of Ameland, The Netherlands, Journal of Coastal Research, 30, 670–684, https://doi.org/10.2112/JCOASTRES-D-13-00125.1, 2014.

de Vries, S., Southgate, H. N., Kanning, W., and Ranasinghe, R.: Dune behavior and aeolian transport on decadal timescales, Coastal Engineering, 67, 41–53, https://doi.org/10.1016/j.coastaleng.2012.04.002, 2012.

Deutscher Wetterdienst: 10-minute station observations of wind for Germany, https://opendata.dwd.de/climate_environment/CDC/observations_germany/climate/10_minutes/wind/historical/.

Döring, M., Walsh, C., and Egberts, L.: "Beyond nature and culture: relational perspectives on the Wadden Sea landscape", Maritime Studies, 20, 225–234, https://doi.org/10.1007/s40152-021-00246-x, 2021.

Du, F. and Jiao, Y.: Mechanical control of plant morphogenesis: concepts and progress, Current opinion in plant biology, 57, 16–23, https://doi.org/10.1016/j.pbi.2020.05.008, 2020.

Duarte, C. M., Losada, I. J., Hendriks, I. E., Mazarrasa, I., and Marbà, N.: The role of coastal plant communities for climate change mitigation and adaptation, Nature Climate Change, 3, 961–968, https://doi.org/10.1038/nclimate1970, 2013.

Everard, M., Jones, L., and Watts, B.: Have we neglected the societal importance of sand dunes? An ecosystem services perspective, Aquatic Conservation: Marine and Freshwater Ecosystems, 20, 476–487, https://doi.org/10.1002/aqc.1114, 2010.

Farrell, E. J., Delgado Fernandez, I., Smyth, T., Li, B., and Swann, C.: Contemporary research in coastal dunes and aeolian processes, Earth Surface Processes and Landforms, https://doi.org/10.1002/esp.5597, 2023.

Feagin, R. A., Figlus, J., Zinnert, J. C., Sigren, J., Martínez, M. L., Silva, R., Smith, W. K., Cox, D., Young, D. R., and Carter, G.: Going with the flow or against the grain? The promise of vegetation for protecting beaches, dunes, and barrier islands from erosion, Frontiers in Ecology and the Environment, 13, 203–210, https://doi.org/10.1890/140218, 2015.

Feagin, R. A., Furman, M., Salgado, K., Martinez, M. L., Innocenti, R. A., Eubanks, K., Figlus, J., Huff, T. P., Sigren, J., and Silva, R.: The role of beach and sand dune vegetation in mediating wave run up erosion, Estuarine, Coastal and Shelf Science, 219, 97–106, https://doi.org/10.1016/j.ecss.2019.01.018, 2019.

Figlus, J.: Designing and implementing coastal dunes for flood risk reduction, in: Coastal Flood Risk Reduction, pp. 287–301, Elsevier, ISBN 9780323852517, https://doi.org/10.1016/B978-0-323-85251-7.00021-4, 2022.

Figlus, J., Kobayashi, N., Gralher, C., and Iranzo, V.: Wave Overtopping and Overwash of Dunes, Journal of Waterway, Port, Coastal, and Ocean Engineering, 137, 26–33, https://doi.org/10.1061/(ASCE)WW.1943-5460.0000060, 2011.

Figlus, J., Sigren, J. M., Armitage, A. R., and Tyler, R. C.: Erosion of vegetated coastal dunes, Coastal Engineering Proceedings, 1, 20, https://doi.org/10.9753/icce.v34.sediment.20, 2014.

Figlus, J., Sigren, J. M., Feagin, R. A., and Armitage, A. R.: The unique ability of fine roots to reduce vegetated coastal dune erosion during wave collision, Frontiers in Built Environment, 8, https://doi.org/10.3389/fbuil.2022.904837, 2022.

Foster-Martinez, M. R., Lacy, J. R., Ferner, M. C., and Variano, E. A.: Wave attenuation across a tidal marsh in San Francisco Bay, Coastal Engineering, 136, 26–40, https://doi.org/10.1016/j.coastaleng.2018.02.001, 2018.

Freschet, G. T. and Roumet, C.: Sampling roots to capture plant and soil functions, Functional Ecology, 31, 1506–1518, https://doi.org/10.1111/1365-2435.12883, 2017.

Gao, J., Kennedy, D. M., and Konlechner, T. M.: Coastal dune mobility over the past century: A global review, Progress in Physical Geography: Earth and Environment, 44, 814–836, https://doi.org/10.1177/0309133320919612, 2020.

Gardiner, B., Berry, P., and Moulia, B.: Review: Wind impacts on plant growth, mechanics and damage, Plant science : an international journal of experimental plant biology, 245, 94–118, https://doi.org/10.1016/j.plantsci.2016.01.006, 2016.

Garzon, J. L., Costas, S., and Ferreira, O.: Biotic and abiotic factors governing dune response to storm events, Earth Surface Processes and Landforms, https://doi.org/10.1002/esp.5300, 2021.

GDWS: Pegel online: Spiekeroog: 9410010, 1, https://www.pegelonline.wsv.de/gast/stammdaten?pegelnr=9410010, 2024.

González-Villanueva, R., Pastoriza, M., Hernández, A., Carballeira, R., Sáez, A., and Bao, R.: Primary drivers of dune cover and shoreline dynamics: A conceptual model based on the Iberian Atlantic coast, Geomorphology, 423, 108 556, https://doi.org/10.1016/j.geomorph.2022.108556, 2023.

Gracia, A., Rangel-Buitrago, N., Oakley, J. A., and Williams, A. T.: Use of ecosystems in coastal erosion management, Ocean & Coastal Management, 156, 277–289, https://doi.org/10.1016/j.ocecoaman.2017.07.009, 2018.

Hacker, S. D., Zarnetske, P., Seabloom, E., Ruggiero, P., Mull, J., Gerrity, S., and Jones, C.: Subtle differences in two non-native congeneric beach grasses significantly affect their colonization, spread, and impact, Oikos, 121, 138–148, https://doi.org/10.1111/j.1600-0706.2011.18887.x, 2012.

Hesp, P.: Foredunes and blowouts: initiation, geomorphology and dynamics, Geomorphology, 48, 245–268, https://doi.org/10.1016/S0169-555X(02)00184-8, 2002.

Hesp, P. A.: The Formation of Shadow Dunes, Journal of Sedimentary Petrology, 51, 101–112, 1981.

Hild, A., Niesel, V., and Günther, C.-P.: Study Area: The Backbarrier Tidal Flats of Spiekeroog, in: The Wadden Sea Ecosystem, edited by Dittmann, S., pp. 15–49, Springer Berlin Heidelberg, Berlin, Heidelberg, ISBN 978-3-642-64256-2, https://doi.org/10.1007/978-3-642-60097-5_3, 1999.

Hovenga, P. A., Ruggiero, P., Goldstein, E. B., Hacker, S. D., and Moore, L. J.: The relative role of constructive and destructive processes in dune evolution on Cape Lookout National Seashore, North Carolina, USA, Earth Surface Processes and Landforms, 46, 2824–2840, https://doi.org/10.1002/esp.5210, 2021.

Huiskes, A. H. L.: Biological Flora of the British isles: Ammophila Arenaria (L.) Link (Psamma Arenaria (L.) Roem. et Schult.; Calamgrostis Arenaria (L.) Roth), Journal of Ecology, 67, 363, https://doi.org/10.2307/2259356, 1979.

Husemann, P., Romão, F., Lima, M., Costas, S., and Coelho, C.: Review of the Quantification of Aeolian Sediment Transport in Coastal Areas, Journal of Marine Science and Engineering, 12, 2024.

Isermann, M.: Patterns in Species Diversity during Succession of Coastal Dunes, Journal of Coastal Research, 27, 661–671, 2011.

Isermann, M. and Cordes, H.: Changes in dune vegetation on Spiekeroog (East Friesian islands) over a 30 year period, in: Coastal Dunes: Geomorphology, Ecology and Management for Conservation., edited by Carter, R., Curtis, T., and Sheehy-Skeffington, M. J., pp. 201–209, Balkema, Rotterdam, 1997.

Keijsers, J., de Groot, A. V., and Riksen, M.: Modeling the biogeomorphic evolution of coastal dunes in response to climate change, Journal of Geophysical Research: Earth Surface, 121, 1161–1181, https://doi.org/10.1002/2015JF003815, 2016.

Keimer, K., Kosmalla, V., Prüter, I., Lojek, O., Prinz, M., Schürenkamp, D., Freund, H., and Goseberg, N.: Proposing a novel classification of growth periods based on biomechanical properties and seasonal changes of Spartina anglica, Frontiers in Marine Science, 10, https://doi.org/10.3389/fmars.2023.1095200, 2023.

Keimer, K., Kind, F., Prüter, I., Kosmalla, V., Lojek, O., Schürenkamp, D., Prinz, M., Niewerth, S., Aberle, J., and Goseberg, N.: From seasonal field study to surrogate modeling: Investigating the biomechanical dynamics of Elymus sp. in salt marshes, Limnology and Oceanography: Methods, https://doi.org/10.1002/lom3.10616, 2024.

Kobayashi, N., Gralher, C., and Do, K.: Effects of Woody Plants on Dune Erosion and Overwash, Journal of Waterway, Port, Coastal, and Ocean Engineering, 139, 466–472, https://doi.org/10.1061/(ASCE)WW.1943-5460.0000200, 2013.

Koch, E. W., Barbier, E. B., Silliman, B. R., Reed, D. J., Perillo, G. M. E., Hacker, S. D., Granek, E. F., Primavera, J. H., Muthiga, N., Polasky, S., Halpern, B. S., Kennedy, C. J., Kappel, C. V., and Wolanski, E.: Non–linearity in ecosystem services: temporal and spatial variability in coastal protection, Frontiers in Ecology and the Environment, 7, 29–37, https://doi.org/10.1890/080126, 2009.

Kosmalla, V., Keimer, K., Ahrenbeck, L., Mehrtens, B., Lojek, O., Schürenkamp, D., and Goseberg, N.: Geometric and mechanical properties dataset of marram grass (Calamagrostis arenaria, formerly Ammophila arenaria) across dune habitats on Spiekeroog Island (December 2021 - December 2022), https://doi.org/10.24355/dbbs.084-202404230724-0, 2024.

Kouhen, M., Dimitrova, A., Scippa, G. S., and Trupiano, D.: The Course of Mechanical Stress: Types, Perception, and Plant Response, Biology, 12, https://doi.org/10.3390/biology12020217, 2023.

LGLN: Digitales Orthophoto (DOP20) [Digital orthophotos]: Landesamt für Geoinformationen und Landesvermessung Niedersachsen [State agency for geoinformation and state survey of Lower Saxony]: Data licence Germany – attribution – Version 2.0, ATKIS, 1, https://ni-lgln-opengeodata.hub.arcgis.com/apps/lgln-opengeodata::digitales-orthophoto-dop20/about, 2024.

Li, C., Peng, Z., Zhao, Y., Fang, D., Chen, X., Xu, F., and Wang, X.: Seasonal variations in drag coefficient of salt marsh vegetation, Coastal Engineering, 193, 104 575, https://doi.org/10.1016/j.coastaleng.2024.104575, 2024.

Liu, J., Kutschke, S., Keimer, K., Kosmalla, V., Schürenkamp, D., Goseberg, N., and Böl, M.: Experimental characterisation and three-dimensional modelling of Elymus for the assessment of ecosystem services, Ecological Engineering, 166, https://doi.org/10.1016/j.ecoleng.2021.106233, 2021.

Martínez, M. L. and Psuty, N. P.: Coastal Dunes: Ecology and Conservation, vol. 171 of *Ecological Studies*, Springer Berlin / Heidelberg, ISBN 9783540740025, 2004.

Maun, M. A.: Adaptations of plants to burial in coastal sand dunes, Canadian Journal of Botany, 76, 713–738, https://doi.org/10.1139/b98-058, 1998.

Maximiliano-Cordova, C., Salgado, K., Martínez, M. L., Mendoza, E., Silva, R., Guevara, R., and Feagin, R. A.: Does the Functional Richness of Plants Reduce Wave Erosion on Embryo Coastal Dunes?, Estuaries and Coasts, 42, 1730–1741, https://doi.org/10.1007/s12237-019-00537-x, 2019.

McGuirk, M. T., Kennedy, D. M., and Konlechner, T.: The Role of Vegetation in Incipient Dune and Foredune Development and Morphology: A Review, Journal of Coastal Research, 38, https://doi.org/10.2112/JCOASTRES-D-21-00021.1, 2022.

Mehrtens, B., Kosmalla, V., Bölker, T., Lojek, O., and Goseberg, N.: Spatial and temporal growth of coastal dune - field observation of the German Wadden Sea Coast, in: Book of abstracts: Building Coastal Resilience 2022, edited by Strypsteen, Glenn, G., Roest, Bart, B., and Rauwoens, Pieter, P., VLIZ Special Publication, https://doi.org/10.48470/28, 2022.

Mehrtens, B., Lojek, O., Kosmalla, V., Bölker, T., and Goseberg, N.: Foredune growth and storm surge protection potential at the Eiderstedt Peninsula, Germany, Frontiers in Marine Science, 9, https://doi.org/10.3389/fmars.2022.1020351, 2023.

Mehrtens, B., Lojek, O., Bölker, T., Ahrenbeck, L., Kosmalla, V., Schweiger, C., Schürenkamp, D., and Goseberg, N.: Experimental Investigation Of Coastal Foredune Erosion, CoastLab 2024: Physical Modelling in Coastal Engineering and Science, https://doi.org/10.59490/coastlab.2024.794, 2024.

Montreuil, A.-L., Bullard, J. E., Chandler, J. H., and Millett, J.: Decadal and seasonal development of embryo dunes on an accreting macrotidal beach: North Lincolnshire, UK, Earth Surface Processes and Landforms, 38, 1851–1868, https://doi.org/10.1002/esp.3432, 2013.

Mostow, R. S., Barreto, F., Biel, R. G., Meyer, E., and Hacker, S. D.: Discovery of a dune–building hybrid beachgrass (Ammophila arenaria × A. breviligulata) in the U.S. Pacific Northwest, Ecosphere, 12, https://doi.org/10.1002/ecs2.3501, 2021.

NLWKN: 80.000 Kubikmeter Sand sollen Spiekeroog schützen, https://www.nlwkn.niedersachsen.de/startseite/aktuelles/presse_und_offentlichkeitsarbeit/pressemitteilungen/80-000-kubikmeter-sand-sollen-spiekeroog-schutzen-223919.html, 14.07.2023.

NLWKN: Digital Elevation Model Spiekeroog: Forschungsstelle Küste, airborne topography survey, 2023, 2023.

Paul, M., Rupprecht, F., Möller, I., Bouma, T. J., Spencer, T., Kudella, M., Wolters, G., van Wesenbeeck, B. K., Jensen, K., Miranda-Lange, M., and Schimmels, S.: Plant stiffness and biomass as drivers for drag forces under extreme wave loading: A flume study on mimics, Coastal Engineering, 117, 70–78, https://doi.org/10.1016/j.coastaleng.2016.07.004, 2016.

Paul, M., Bischoff, C., and Koop-Jakobsen, K.: Biomechanical traits of salt marsh vegetation are insensitive to future climate scenarios, Scientific Reports, 12, 21 272, https://doi.org/10.1038/s41598-022-25525-3, 2022.

Pickart, A. J.: Ammophila invasion ecology and dune restoration on the west coast of North America, Diversity, 13, 629, https://doi.org/10.3390/d13120629, 2021.

Pollmann, T., Junge, B., and Giani, L.: Landscapes and soils of North Sea barrier islands: A comparative analysis of the old west and young east of Spiekeroog island (Germany), Erdkunde, 72, 273–286, 2018.

Pott, R.: Die Pflanzengesellschaften Deutschlands, vol. 8067 of *UTB für Wissenschaft Große Reihe Botanik, Ökologie, Agrar- und Forstwissenschaften*, Ulmer, Stuttgart, 2., überarb. und stark erw. aufl. edn., ISBN 9783825280673, 1995.

Puijalon, S., Bornette, G., and Sagnes, P.: Adaptations to increasing hydraulic stress: morphology, hydrodynamics and fitness of two higher aquatic plant species, Journal of Experimental Botany, 56, 777–786, https://doi.org/10.1093/jxb/eri063, 2005.

Puijalon, S., Bouma, T. J., Douady, C. J., van Groenendael, J., Anten, N., Martel, E., and Bornette, G.: Plant resistance to mechanical stress: evidence of an avoidance-tolerance trade-off, New Phytologist, 191, 1141–1149, https://doi.org/10.1111/j.1469-8137.2011.03763.x, 2011.

Pye, K. and Blott, S. J.: Assessment of beach and dune erosion and accretion using LiDAR: Impact of the stormy 2013–14 winter and longer term trends on the Sefton Coast, UK, Geomorphology, 266, 146–167, https://doi.org/10.1016/j.geomorph.2016.05.011, 2016.

Rader, A. M., Pickart, A. J., Walker, I. J., Hesp, P. A., and Bauer, B. O.: Foredune morphodynamics and sediment budgets at seasonal to decadal scales: Humboldt Bay National Wildlife Refuge, California, USA, Geomorphology, 318, 69–87, https://doi.org/10.1016/j.geomorph.2018.06.003, 2018.

Röper, T., Greskowiak, J., Freund, H., and Massmann, G.: Freshwater lens formation below juvenile dunes on a barrier island (Spiekeroog, Northwest Germany), Estuarine, Coastal and Shelf Science, 121-122, 40–50, https://doi.org/10.1016/j.ecss.2013.02.004, 2013.

Ruggiero, P., Hacker, S., Seabloom, E., and Zarnetske, P.: The Role of Vegetation in Determining Dune Morphology, Exposure to Sea-Level Rise, and Storm-Induced Coastal Hazards: A U.S. Pacific Northwest Perspective, in: Barrier Dynamics and Response to Changing Climate, edited by Moore, L. J. and Murray, A. B., pp. 337–361, Springer International Publishing, Cham, ISBN 978-3-319-68084-2, https://doi.org/10.1007/978-3-319-68086-6_11, 2018.

Rupprecht, F., Möller, I., Evans, B., Spencer, T., and Jensen, K.: Biophysical properties of salt marsh canopies - Quantifying plant stem flexibility and above ground biomass, Coastal Engineering, 100, 48–57, https://doi.org/10.1016/j.coastaleng.2015.03.009, 2015.

Rupprecht, F., Möller, I., Paul, M., Kudella, M., Spencer, T., van Wesenbeeck, B. K., Wolters, G., Jensen, K., Bouma, T. J., Miranda-Lange, M., and Schimmels, S.: Vegetation-wave interactions in salt marshes under storm surge conditions, Ecological Engineering, 100, 301–315, https://doi.org/10.1016/j.ecoleng.2016.12.030, 2017.

Scanntronik Mugrauer GmbH: Thermofox and Hygrofox: Operating instructions, https://www.scanntronik.de/English/Manual%20for%20the%20Hygrofox%20and%20Thermofox%20Universal.pdf, 2024a.

Scanntronik Mugrauer GmbH: Data sheet for: Soil Analysis Sensor (Digital) + Analog Soil Sensor, Revision 2.0, https://www.scanntronik.de/English/Soil%20Sensor%20-%20Datasheet.pdf, 2024b.

Schulze, D., Rupprecht, F., Nolte, S., and Jensen, K.: Seasonal and spatial within-marsh differences of biophysical plant properties: implications for wave attenuation capacity of salt marshes, Aquatic Sciences, 81, 65, https://doi.org/10.1007/s00027-019-0660-1, 2019.

Schweiger, C. and Schuettrumpf, H.: Considering the Effect of Land-Based Biomass on Dune Erosion Volumes in Large-Scale Numerical Modeling, Journal of Marine Science and Engineering, 9, 843, https://doi.org/10.3390/jmse9080843, 2021.

Seabloom, E. W. and Wiedemann, A. M.: Distribution and effects of Ammophila breviligulata Fern. (American Beachgrass) on the foredunes of the Washington coast, Journal of Coastal Research, 10, 178–188, 1994.

Shepard, C. C., Crain, C. M., and Beck, M. W.: The protective role of coastal marshes: a systematic review and meta-analysis, PloS one, 6, e27 374, https://doi.org/10.1371/journal.pone.0027374, 2011.

Silva, R., Martínez, M. L., Odériz, I., Mendoza, E., and Feagin, R. A.: Response of vegetated dune–beach systems to storm conditions, Coastal Engineering, 109, 53–62, https://doi.org/10.1016/j.coastaleng.2015.12.007, 2016.

Stalter, R. and Lonard, R. I.: Biological flora of sand dunes on the Northwest Pacific coastline of North America: Ammophila arenaria (L.) Link and Ammophila breviligulata Fernald, Journal of Coastal Research, 40, 994–1000, https://doi.org/10.2112/JCOASTRES-D-24A-00003.1, 2024.

Strypsteen, G., Houthuys, R., and Rauwoens, P.: Dune Volume Changes at Decadal Timescales and Its Relation with Potential Aeolian Transport, Journal of Marine Science and Engineering, 7, 357, https://doi.org/10.3390/jmse7100357, 2019.

Strypsteen, G., Delgado-Fernandez, I., Derijckere, J., and Rauwoens, P.: Fetch–driven aeolian sediment transport on a sandy beach: A new study, Earth Surface Processes and Landforms, https://doi.org/10.1002/esp.5784, 2024.

Telewski, F. W.: Thigmomorphogenesis: the response of plants to mechanical perturbation, Italus Hortus, 23, 1–16, 2016.

Tomasicchio, G. R., Sánchez-Arcilla, A., D'Alessandro, F., Ilic, S., James, M. R., Sancho, F., Fortes, C. J., and Schüttrumpf, H.: Large-scale experiments on dune erosion processes, Journal of Hydraulic Research, 49, 20–30, https://doi.org/10.1080/00221686.2011.604574, 2011.

Türker, U., Yagci, O., and Kabdasli, M. S.: Impact of nearshore vegetation on coastal dune erosion: assessment through laboratory experiments, Environmental Earth Sciences, 78, https://doi.org/10.1007/s12665-019-8602-8, 2019.

van der Putten, W. H. and Troelstra, S. R.: Harmful soil organisms in coastal foredunes involved in degeneration of Ammophila arenaria and Calammophila baltica, Canadian Journal of Botany, 68, 1560–1568, 1990.

van Gent, M. R. A., Coeveld, E. M., de Vroeg, H., and van de Graaff, J.: Dune erosion prediction methods incorporating effects of wave periods, Coastal Sediments 2007 Conference Paper, pp. 612–625, https://doi.org/10.1061/40926(239)46, 2007.

van Gent, M. R. A., van Thiel de Vries, J., Coeveld, E. M., de Vroeg, J. H., and van de Graaff, J.: Large-scale dune erosion tests to study the influence of wave periods, Coastal Engineering, 55, 1041–1051, https://doi.org/10.1016/j.coastaleng.2008.04.003, 2008.

van IJzendoorn, C. O., de Vries, S., Hallin, C., and Hesp, P. A.: Sea level rise outpaced by vertical dune toe translation on prograding coasts, Scientific Reports, 11, 12 792, https://doi.org/10.1038/s41598-021-92150-x, 2021.

van Rijn, L. C. and Strypsteen, G.: A fully predictive model for aeolian sand transport, Coastal Engineering, 156, 103 600, https://doi.org/10.1016/j.coastaleng.2019.103600, 2020.

van Westen, B., de Vries, S., Cohn, N., van IJzendoorn, C., Strypsteen, G., and Hallin, C.: AeoLiS: Numerical modelling of coastal dunes and aeolian landform development for real-world applications, Environmental Modelling & Software, 179, 106 093, https://doi.org/10.1016/j.envsoft.2024.106093, 2024.

Vuik, V., Suh Heo, H. Y., Zhu, Z., Borsje, B. W., and Jonkman, S. N.: Stem breakage of salt marsh vegetation under wave forcing: A field and model study, Estuarine, Coastal and Shelf Science, 200, 41–58, https://doi.org/10.1016/j.ecss.2017.09.028, 2017.

Walker, S. L. and Zinnert, J.: Whole plant traits of coastal dune vegetation and implications for interactions with dune dynamics, Ecosphere, 13, https://doi.org/10.1002/ecs2.4065, 2022.

Zarnetske, P. L., Hacker, S. D., Seabloom, E. W., Ruggiero, P., Killian, J. R., Maddux, T. B., and Cox, D.: Biophysical feedback mediates effects of invasive grasses on coastal dune shape, Ecology, 93, 1439–1450, https://doi.org/10.1890/11-1112.1, 2012.

Zarnetske, P. L., Ruggiero, P., Seabloom, E. W., and Hacker, S. D.: Coastal foredune evolution: the relative influence of vegetation and sand supply in the US Pacific Northwest, Journal of the Royal Society, Interface, 12, https://doi.org/10.1098/rsif.2015.0017, 2015.

Zhu, Z., Yang, Z., and Bouma, T. J.: Biomechanical properties of marsh vegetation in space and time: effects of salinity, inundation and seasonality, Annals of Botany, 125, 277–290, https://doi.org/10.1093/aob/mcz063, 2020.

ZwickRoell GmbH & Co.KG: Product Information: Materials Testing Machines zwickiLine Z0.5 to Z5.0, https://www.zwickroell.com/fileadmin/content/Files/SharePoint/user_upload/PI_EN/02_396_zwickiLine_Z0_5_up_to_Z5_0_Materials_Testing_Machine_PI_EN.pdf, 2024.